Antoni Rullan de la Cruz

Evaluation of Innovative Approaches in Active Distribution Network Management via Time-Series Simulations

Master Thesis
PSL1514

EEH – Power Systems Laboratory
Swiss Federal Institute of Technology (ETH) Zurich

Examiner: Prof. Dr. Göran Andersson
Supervisor: Dr. Stephan Koch

Zurich, September 28, 2015

Abstract

European directives for renewable energies and decreasing costs of these alternative generation technologies are incentivising a transformation of the electricity markets, grid infrastructure and the way the grid is operated. Distribution networks, which were not traditionally designed to host generation, have to deal now with distributed energy resources that feed intermittent power into the grid. Thus, due to the fact that excess energy from these intermittent sources cannot be hosted, not only the need of energy storage in power systems has emerged but also of new control strategies in the field of grid planning such as demand response or curtailment of generation units.

In order to take SmartGrid elements and control strategies into the planning stage, the ETH Zurich spin-off Adaptricity has developed DPG.sim, a time-series simulation software that can overcome traditional grid planning software limitations in representing the behavior of SmartGrid elements for grid planning studies.

Within the traditional grid extension planning, this thesis addresses the implementation of an automatic grid upgrade algorithm to be used with DPG.sim to automatically select which elements must be substituted. This work also demonstrates, using temporal simulations in DPG.sim, the scope of active network management strategies to enlarge grid hosting capacity of distributed energy generation. Thus, it will show how these strategies can reduce the technical challenges faced by Distribution System Operators (DSOs) such as overvoltages and line overloadings.

Keywords: time-series simulation, benchmark grids, active network management, photovoltaics, wind power, energy storage, demand response, automatic grid planning algorithm.

Acknowledgements

This project has been an interesting journey into the world of grid planning and smart-grid challenges within the framework of a generic and multidisciplinary Engineer's degree, a journey that does not seem to finish with this report. I really appreciate not only the opportunity given by the Polytechnic University of Barcelona (UPC) and the ETH Zurich to study 1 year in Zurich but also to carry out my final thesis at the ETH spin-off Adaptricity. I have always found very interesting to gain experience in the private sector before I had finished my degree. I also want to thank my supervisor, Stephan, for his guidance and especially for his patience to answer my questions.

My deepest gratitude goes to my parents who have been guiding, educating and supporting me the best they have known and for as long as I can remember. And they still do. I cannot conclude without warmly thanking my grandmother, Carmina, for her endless support, generosity and care and my girlfriend, Amelia, for being always by my side and encouraging me during this stay in Zurich on hundreds of conversations over Skype.

Contents

List of Acronyms

ANM Active Network Management

BESS Battery Energy Storage System

DER Distributed Energy Resources

DR Demand Response

DSO Distribution System Operators

EU European Union

LV Low Voltage

MV Medium Voltage

OLTC On-Load Tap-Changing

PV Photovoltaic

Chapter 1

Introduction

The share of energy generated from renewable sources in the European grid has strongly increased and is challenging European utilities. The European Union (EU) directive for the promotion of renewable energies sets a target of 20% in final energy consumption from renewable sources by 2020. To achieve this, EU countries have committed to reaching their own national targets ranging from 10% in Malta to 49% in Sweden. Gross electricity generation from renewable energies is on a long-term increasing trend: between 1990 and 2013 it has almost tripled as shown in Fig. 1.1 [1].

Fig. 1.2 shows that this rise is even much higher if the share of hydro power is not taken into account. For instance, the average annual growth rate of PV has been 68.5% over the last five years. Photovoltaic energy is currently the third most important form of renewable energy in terms of capacity, only behind hydropower and wind. As of 2014, 177 GW of PV capacity is installed across the world [2]. Due to EU incentive scheme and decreasing costs of these technologies, the use of solar energy (which already represents a 10% of renewable production) and wind energy should increase. As a result of these changes in energy production, the way the energy is fed into the grid is changing from centralized generation of large power plants to more decentralized generation from distributed energy resources (DER).

Firstly, distribution networks were not traditionally designed to host generation, because energy was generated in a more centralized way and then transported to the distribution grid. Besides, and due to the unbundling between distribution system operators and power production, DSOs cannot freely decide on the location, size or connection time of distributed generation (DG), which causes more uncertainties for the DSO to make long-term network planning. The technical challenges faced by the DSO include overvoltages in low and medium voltage grids as well as unwanted backflows into the upper voltage levels due to power in-feed from DG. The quick growth

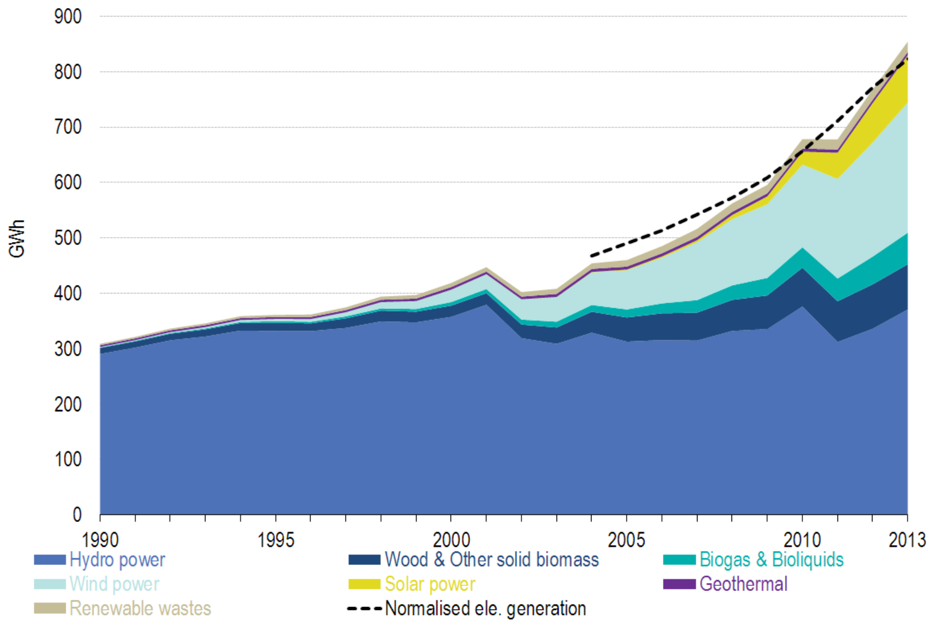

Source: Eurostat

Figure 1.1: Gross electricity generation from renewable sources, EU-28, 1990-2013.

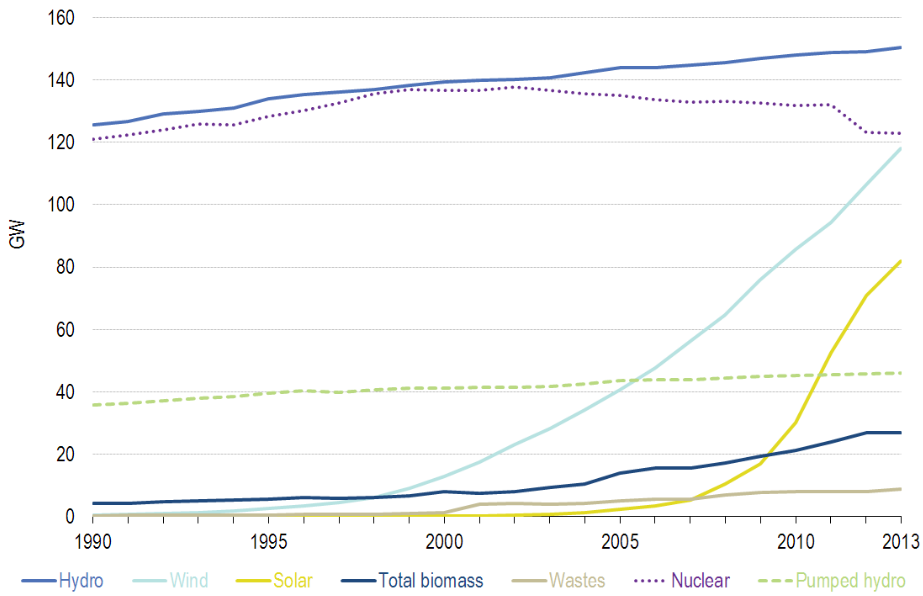

Source: Eurostat

Figure 1.2: Electricity generation capacity, EU-28, 1990-2013.

of energy generation in the domestic sector leads to the input of energy into low voltage networks in residential areas (around 80% of PV power is fed into the Low-Voltage (LV) distribution grid and 15% into the medium voltage level [3]), which may overload power lines and transformers in certain cases. Moreover, as renewable energy sources such as PV or wind do not deliver power constantly, there is a bigger need for load balancing of energy consumption and generation to ensure power quality. DG can also be challenging with respect to harmonics.

With the ambitious renewable generation targets for the European countries for the next few decades, many promising alternatives to conventional grid reinforcements have been proposed to increase the hosting capacity of DG in LV distribution grids. If these SmartGrid approaches allow to make further use of existing infrastructure, the high costs of grid reinforcement and expansion could be avoided. Several solutions are outlined below:

- Reactive power control: Localized consumption of reactive power in presence of an active power in-feed, e.g. by PV panels, has proved to decrease the node voltage [4]. However, decentralized consumption can also help [5].
- On-Load Tap-Changing Transformers: Transformers can be fitted with an on-load tap-changing (OLTC) mechanism to ensure continuous power supply while enabling stepped voltage regulation of the secondary side of the transformer [5].
- Curtailment of active power generation: Although it has some economic impact for producers because less energy is generated, it is often used due to ease of use (especially in emergency situations) .
- Energy storage: Battery Energy Storage Systems (BESS) can be used to reduce demand peaks, to provide frequency control reserve and balance short-term fluctuations between stochastic consumption and intermittent, uneven generation [6].
- Demand Response (DR): Water heaters or electrical vehicles can be activated to consume electrical power when there is a generation peak, in order to maximize use of local energy and avoid unwanted backflows [7].

Simulations are an essential tool for network planning and to investigate active network management approaches to increase hosting capacity of DG without upgrading the grid. Traditional distribution grid planning is usually based on the worst case scenario where the maximum coincident load is connected and snapshot simulations can be carried out. When a large amount of distributed generation is connected, the scenario where the maximum coincident generation is produced can even require a larger infrastructure reinforcement. However, addressing the network planning via worst-case scenarios can lead to over-dimensioned networks without effectively making use of the existent grid.

A simulation software DPG.sim is developed by the ETH Zürich spin-off Adaptricity [8]. DPG.sim takes into account active network management strategies and SmartGrid elements in the grid planning stage, in order not to over-dimension the existent grid and therefore reducing investment costs. The software can run temporal simulations of distributed generation, load and storage while integrating control strategies for the user to assess the result of his planning strategies and SmartGrid elements.

1.1 Objectives and scope of the master thesis

Within this master's thesis, DPG.sim shall be used for the generation of benchmark simulation cases that demonstrate the benefits of active network management (ANM) approaches.

As a first approach, a number of benchmark simulation cases of different scales (individual low-voltage network, individual medium-voltage feeder, rural distribution network) are constructed in DPG.sim. This comprises the selection of a proper network topology and the definition of dispersed load, generation and storage units within the prosumers (electricity consumers that are also producers) in the grid. A special focus is given to distributed renewable energy sources. These scenarios are used to identify situations where ANM approaches are needed. Then, mitigation strategies that are implementable in DPG.sim shall be tested for the various situations. System characteristics are also analysed and evaluated for judging the suitability of the various available approaches. Alternatively, an algorithm for conventional grid reinforcement to substitute and upgrade the appropriate lines and transformers of the grid is also developed to make the traditional expansion automatic.

1.2 Thesis outline

The thesis is divided in the following chapters:

- Chapter 2 explains the procedure to model prosumers in DPG.sim.
- Chapter 3 details the units models used in the study (parameterization, variables, equations and other attributes).

- Chapter 4 details the three benchmark grids where the prosumers will be dispersed.
- Chapter 5 presents the voltages and loadings over the simulation period of the grids listed in Chapter 4.
- Chapter 6 introduces the technical requirements and operation strategies for the simulations.
- Chapter 7 presents the results of the simulations.
- Chapter 8 describes how the automatic planning algorithm works and provides an example of applying the algorithm to a MV benchmark grid.
- Chapter 9 concludes the work and gives some ideas for future studies.

Chapter 2

Prosumer Modelling

In this chapter, the way prosumers are modelled is detailed. The prosumers include units and stochastic data sets associated to these units. The Fig. 2.1 shows this relation between prosumers and units and how each prosumer is then connected to the grid. First, unit modelling is introduced and then the associated stochastic dataset.

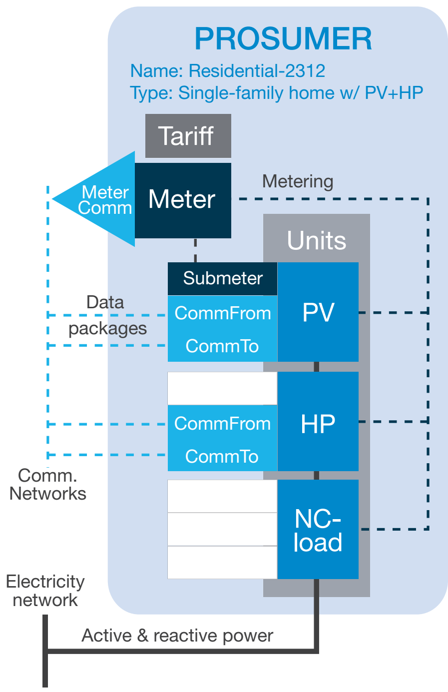

Source: Adaptricity

Figure 2.1: Prosumer representation connected to the grid in DPG.sim.

2.1 Units

This section introduces unit modelling, including unit variables, equations and controller modelling and reactive power characteristic. The units are classified in static and dynamic units. Dynamic units have an intrinsic energy storage or internal state that represents an inter-temporal relation between time steps (e.g. thermal units) and static units interact with the grid just by a consumption or generation behaviour that may be determined by a time series (e.g. non-controllable load units).

Unit parameters

To characterize each unit, the following four types of parameter and variables are used:

- Unit parameters, which are constant values for each unit, such as efficiency and rated power capacity or energy storage capacity.
- Input variables, which have external influences or are controlled internally and their values will influence either the system state or the system output. Some examples could be power generation on a PV unit (changes due to external influences).
- Output variables are those that can be measured either internally or externally, for instance energy stored in a battery or electrical power consumption. An input variable can be at the same time a measurable (i.e. output) variable.
- State variables are just specified for dynamic units. This variable represents an inter-temporal relation between time steps of a dynamic unit's internal state, e.g. state of charge of a battery or inner temperature of a thermal load.

Model equations

- Dynamic units are the ones that have one or more state variables. The inter-temporal relation between time steps is determined by the following state equation:

  $$\dot{x} = A \cdot (x - x_{\mathrm{ss}}) + B \cdot u$$

  where x is the state variables vector, u is the input vector, A is the dynamic matrix and B the input matrix. x_{ss} is the steady state value that works as an offset for this linear equation, e.g. ambient temperature for a thermal load. The initial state of x, i.e. initial condition x_0, will also be set.

The outputs that can be measured either by a controller inside the unit or a communication interface to the outside are described by the output equation:

$$y = C \cdot x + D \cdot u$$

where y is the output vector, C is the state output matrix and D is the feed-through matrix.

- Static units do not have the mentioned internal state and therefore no state variable:

  $$\dot{x} = x = 0$$

  Thus, the model equations yield:

  $$B \cdot u = 0$$

  $$y = D \cdot u$$

  The first equation interrelates the input variables and the second links the output with the input variables. Once the previously mentioned vectors and equations are already set, installed load, generation and storage capacity parameters must be identified as well as the power generation and consumption variables for the software to know how much power infeed or outtake there is.

Reactive power characteristic

To conclude, the reactive power characteristic of the units must be defined with one of the following options: Fixed or fluctuating Q, fixed or fluctuating cos ϕ, and Q or cos ϕ as a function of load P.

Unit controllers

Internal and/or external control operation can be described as follows.

- Internal controller: Both the input variable to be controlled and the output variable on which this input depends will be selected. Internal controller parameters such as temperature set-point can also be defined. Then the operation of the hysteresis control algorithm has to be defined.

- External controller: not only controllable input variables but also measurable variables from outside shall be selected. The value of these controllable input variables can be modified from an external interface.

2.2 Stochastic Data Sets

This section introduces briefly how the numerical data and associated time-series are included in the prosumer objects.

Time Series

A csv file with temporal data points and the corresponding value of a variable shall be imported and the amount of time between each data point introduced. The time series used for the load and generation units are presented in the appendix A.

Numerical parameters introduction

So far, no numerical values for the unit parameters have been defined. However, appropriate distributions for each parameter have to be set as well as the imported time-series have to be associated to unit states and input variables. The following distributions can be chosen for each unit parameter: deterministic, uniform, normal, exponential and Poisson.

2.3 Prosumers

Once the above-mentioned models have been introduced, the prosumers to be dispersed into the grid shall be modelled, associating each unit model with its corresponding stochastic dataset, yielding what is represented in Fig. 2.1.

Chapter 3

Unit Models

The units models used in the simulations are presented in this chapter.

3.1 Thermal load

Within this section, the equations, variables and parameters of the water heaters used in some scenarios are detailed.

Unit Parameters:

Variable	**Description**	**Unit**
m	Mass within device	kg
c_{bar}	Average heat capacity	$\mathrm{kJ/(kg \cdot {}^{\circ}C)}$
A	Hull surface area	$\mathrm{m^2}$
h_{bar}	Average heat transfer coefficient	$\mathrm{kW/(m^2 \cdot {}^{\circ}C)}$
P_{rat}	Rated power demand	kW
η_{elec}	Electrical efficiency	$-$

Input variables:

u_{switch}	Appliance on/off mode	$-$

Output variables:

T_{int}	Internal temperature	°C

State variables:

T_{int}	Internal temperature	°C

Dynamic equation:

$dT_{\text{int}}/dt = (A \cdot h_{\text{bar}})/(m \cdot c_{\text{bar}}) \cdot (T_{\text{amb}} - T_{\text{int}}) - (\eta_{\text{elec}} \cdot P_{\text{rat}})/(m \cdot c_{\text{bar}}) \cdot u_{\text{switch}}$

Reactive power properties: Fixed $\cos(\phi) = 1$

3.2 Non-controllable load

The basic parameterization of non-controllable loads to be attached, for instance, with each household prosumer is explained as follows:

Unit Parameters:

Variable	**Description**	**Unit**
P_{rat}	Installed capacity	kW

Input variables:

P_{load}	Electrical load	kW
ξ	Consumption (negative)	–

Output variables:

P_{load}	Electrical load	kW

Output equations:

$$P_{\text{load}} = P_{\text{rat}} \cdot \xi$$

Reactive power properties: Fixed $\cos(\phi) = 0.98$

3.3 Industry load

The industry load is virtually the same as a non-controllable load with a lower inductive $\cos(\phi)$.

Unit Parameters:

Variable	Description	Unit
P_{rat}	Installed capacity	kW

Input variables:

P_{load}	Electrical load	kW
ξ	Consumption (negative)	–

Output variables:

P_{load}	Electrical load	kW

Output equations:

$$P_{\text{load}} = P_{\text{rat}} \cdot \xi$$

Reactive power properties: Fixed $\cos(\phi) = 0.9$

3.4 Battery unit

The modelling of storage units to be used in the simulations is described in this section.

Unit Parameters:

Variable	Description	Unit
C	Storage capacity	kWh
η_{load}	Charging efficiency	–
η_{gen}	Injection efficiency	–
$P_{\text{load}}^{\text{rat}}$	Rated power demand	kW
$P_{\text{gen}}^{\text{rat}}$	Rated power injection	kW

Input variables:

u_{load}	Charging input	–
u_{gen}	Injection input	–

Output variables:

E_{soc}	Available energy	kWh
P_{load}	Charging power	kW
P_{gen}	Discharging power	kW

State variables:

x_{soc}	State of charge	$-$

Dynamic equation:

$$dx_{\text{soc}}/dt = (\eta_{\text{load}} \cdot P^{\text{rat}}_{\text{load}})/C \cdot u_{\text{load}} - P^{\text{rat}}_{\text{gen}}/(C \cdot \eta_{\text{gen}}) \cdot u_{\text{gen}}$$

Output equations:

$$E_{\text{soc}} = \mathrm{C} \cdot \mathrm{x}_{\text{soc}}$$
$$P_{\text{load}} = P^{\text{rat}}_{\text{load}} \cdot u_{\text{load}}$$
$$E_{\text{gen}} = P^{\text{rat}}_{\text{gen}} \cdot u_{\text{gen}}$$

Reactive power properties: Fixed $\cos(\phi) = 1$

3.5 PV Unit

This section details the parameterization of PV units.

Unit Parameters:

Variable	**Description**	**Unit**
P_{rat}	Installed capacity	kW
η	Efficiency	$-$

Input variables:

P_{gen}	Electrical generation	kW
ξ	PV input	$-$
w	Curtailment	$-$

Output variables:

P_{gen}	Electrical generation	kW
P_{curt}	Curtailment power	kW

Output equations:

$$P_{\text{gen}} = P_{\text{rat}} \cdot \eta \cdot (\xi - w)$$
$$P_{\text{curt}} = P_{\text{rat}} \cdot \eta \cdot w$$

Reactive power properties: Fixed $\cos(\phi) = 1$

3.6 Wind Unit

The parameterization of wind units can be found in this section and is virtually identical to the PV units.

Unit Parameters:

Variable	**Description**	**Unit**
P_{rat}	Installed capacity	kW
η	Efficiency	–

Input variables:

P_{gen}	Electrical generation	kW
ξ	PV input	–
w	Curtailment	–

Output variables:

P_{gen}	Electrical generation	kW
P_{curt}	Curtailment power	kW

Output equations:

$$P_{\text{gen}} = P_{\text{rat}} \cdot \eta \cdot (\xi - w)$$

$$P_{\text{curt}} = P_{\text{rat}} \cdot \eta \cdot w$$

Reactive power properties: Fixed $\cos(\phi) = 1$

Chapter 4

Benchmark grids

In order to test active network management strategies in distributions grids, some benchmark grids are needed to develop different scenarios. Three different benchmark grids have been selected from the available literature, including CIGRE Task Force C6.04.02 “Computational Tools and Techniques for Analysis, Design and Validation of Distributed Generation Systems”, which proposes some networks to test techniques that facilitate the integration of DG. The capacity of the lines or transformers of the grids where this data was not provided were derived from similar lines (in terms of resistance, reactance or capacitance) of a well-known cable supplier.

4.1 Low Voltage Benchmark Microgrid

The presented LV microgrid comes from CIGRE TF C6.04.02 [9]. The lines are underground cables (mainly found in urban areas with a high load density) and overhead lines. The parameters of the grid are presented in Tables 4.1, 4.2 and 4.3 and the sketch of the LV network is presented in Fig. 4.1. The two weakest transformers were upgraded from the original parametrization due to the big amount of DG that is planned to be dispersed. As it can be seen, the topology is also radial.

4.2 Rural MV Benchmark Distribution Grid

The MV rural distribution network benchmark is derived from a German MV distribution network which has rural character and supplies a small town and the surrounding rural area. The number of nodes was reduced

Table 4.1: Buses list of the LV benchmark distribution grid.

Name	**Voltage (kV)**	**Type of load**
R0	20	-
R1	0.4	Residential
R2	0.4	Residential
R3	0.4	Residential
R4	0.4	Residential
R5	0.4	Residential
R6	0.4	Residential
R7	0.4	Residential
R8	0.4	Residential
R9	0.4	Residential
R10	0.4	Residential
R11	0.4	Residential
R12	0.4	Residential
R13	0.4	Residential
R14	0.4	Residential
R15	0.4	Residential
R16	0.4	Residential
R17	0.4	Residential
R18	0.4	Residential
I1	0.4	Industrial
I2	0.4	Industrial
C1	0.4	Commercial
C2	0.4	Commercial
C3	0.4	Commercial
C4	0.4	Commercial
C5	0.4	Commercial
C6	0.4	Commercial
C7	0.4	Commercial
C8	0.4	Commercial
C9	0.4	Commercial
C10	0.4	Commercial
C11	0.4	Commercial
C12	0.4	Commercial
C13	0.4	Commercial
C14	0.4	Commercial
C15	0.4	Commercial
C16	0.4	Commercial
C17	0.4	Commercial
C18	0.4	Commercial
C19	0.4	Commercial
C20	0.4	Commercial
C21	0.4	Commercial

Table 4.2: Line parameters of the LV benchmark distribution grid.

From bus	**To bus**	**Length (km)**	**Resistance (Ω/km)**	**Reactance (Ω/km)**	$\mathbf{I}_{max}$ **(A)**
R1	R2	0.035	0.284	0.083	318
R2	R3	0.035	0.284	0.083	318
R3	R4	0.035	0.284	0.083	318
R3	R11	0.03	3.69	0.094	49
R4	R5	0.035	0.284	0.083	318
R4	R12	0.035	0.497	0.086	193
R5	R6	0.035	0.284	0.083	318
R6	R7	0.035	0.284	0.083	318
R6	R16	0.03	0.871	0.081	134
R7	R8	0.035	0.284	0.083	318
R8	R9	0.035	0.284	0.083	318
R9	R10	0.035	0.284	0.083	318
R9	R17	0.03	3.69	0.094	49
R10	R18	0.03	1.38	0.082	101
R12	R13	0.035	0.497	0.086	193
R13	R14	0.035	0.497	0.086	193
R14	R15	0.03	0.822	0.077	199
I1	I2	0.2	0.264	0.071	254
C1	C2	0.03	0.397	0.279	199
C2	C3	0.03	0.397	0.279	199
C3	C4	0.03	0.397	0.279	199
C3	C10	0.03	0.574	0.294	140
C3	C21	0.03	0.41	0.071	240
C4	C5	0.03	0.397	0.279	199
C5	C6	0.03	0.574	0.294	140
C5	C15	0.03	1.218	0.318	101
C6	C7	0.03	0.574	0.294	140
C7	C8	0.03	0.574	0.294	140
C8	C9	0.03	0.574	0.294	140
C8	C19	0.03	0.41	0.071	240
C9	C20	0.03	0.41	0.071	240
C10	C11	0.03	0.574	0.294	140
C10	C14	0.03	0.41	0.071	240
C11	C12	0.03	0.41	0.071	240
C11	C13	0.03	0.41	0.071	240
C15	C16	0.03	1.218	0.318	101
C15	C18	0.03	0.41	0.071	240
C16	C17	0.03	0.41	0.071	240

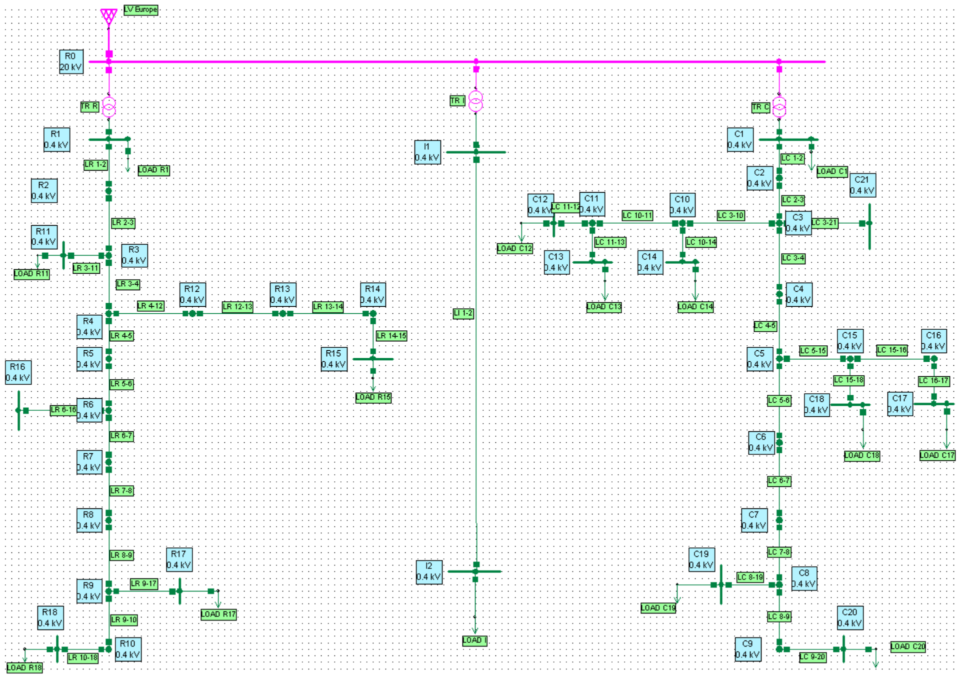

Figure 4.1: Sketch of the LV benchmark distribution grid.

Table 4.3: Transformers parameters of the LV benchmark distribution grid.

From bus	To bus	Rated power (MVA)	Voltage1 (kV)	Voltage2 (kV)	U_k (%)	U_r (%)
218660	218732	0.5	20	0.4	4.13	1.002
218660	218947	0.5	20	0.4	4.1	1.0
218660	218985	0.55	20	0.4	4.09	0.993

in order to yield a simplified test case for DG integration studies [10]. The rated voltage level of the network is 20 kV and it is supplied from a 110 kV transformer. Most connections are made with cables, but there are also some overhead lines.

The parameters that characterise lines, transformers and buses of the distribution grid are detailed in Tables 4.4, 4.5 and 4.6 and the sketch of the network is presented in Fig. 4.2. As it can be seen, the topology is radial.

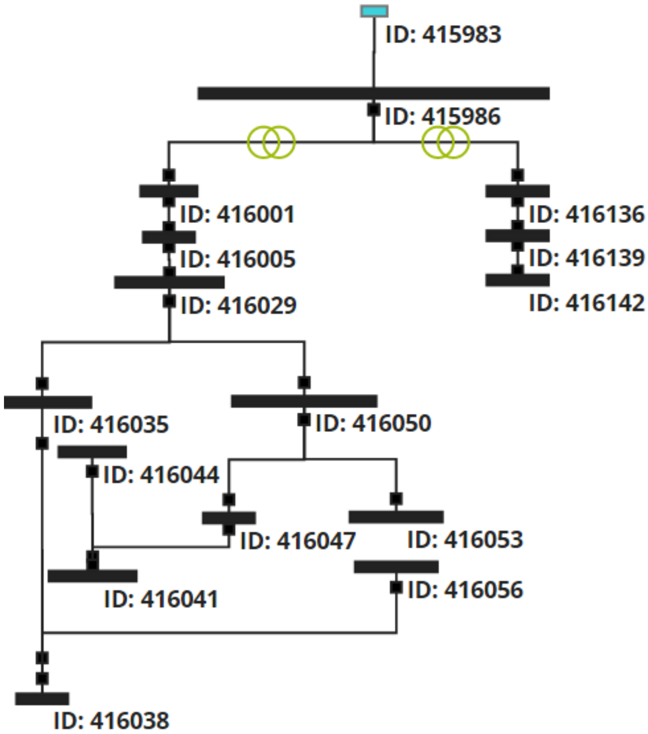

Figure 4.2: Sketch of the MV rural benchmark distribution grid.

Table 4.4: Buses list of the MV Rural benchmark distribution grid.

Bus name	**Voltage (kV)**	**Type of load**
415986	110	-
416001	20	Residential
416005	20	Residential
416029	20	Residential
416035	20	Residential
416038	20	Residential
416056	20	Residential
416050	20	Residential
416047	20	Residential
416041	20	Residential
416044	20	Residential
416053	20	Residential
416136	20	Industrial
416139	20	Industrial
416142	20	Industrial

Table 4.5: Line parameters of the MV Rural benchmark distribution grid.

From bus	To bus	Length (km)	Resistance (Ω/km)	Reactance (Ω/km)	Capacitance (μF/km)	I_{max} (A)
416001	416005	2.82	0.579	0.367	0.15888	310
416029	416035	0.61	0.262	0.121	0.648	220
416044	416041	0.33	0.367	0.133	0.456	170
416041	416047	0.77	0.339	0.133	0.4832	170
416035	416038	0.56	0.354	0.129	0.456	170
416005	416029	4.42	0.164	0.113	0.6608	310
416050	416053	1.67	0.294	0.123	0.56	220
416047	416050	0.32	0.339	0.13	0.4368	170
416038	416056	1.54	0.336	0.126	0.5488	170
416136	416139	4.89	0.337	0.358	0.16288	292
416139	416142	2.99	0.202	0.122	0.4784	220

Table 4.6: Transformers parameters of the MV rural benchmark distribution grid.

From bus	To bus	Rated power (MVA)	Voltage1 (kV)	Voltage2 (kV)	U_k (%)	U_r (%)
415986	416001	42.7289	110	20	12.5	0.56
415986	416136	42.7289	110	20	12.5	0.56

4.3 Urban MV Benchmark Distribution Grid

The following 75-bus MV Distribution Grid for comparing Active Network Management strategies comes from [11]. Tables 4.7 and 4.8 include the parameters that characterise grid lines and transformers. The only transformer of the grid is also upgraded to withstand more power, as it was undersized for the amount of generation in scenarios to be studied. The topology of the grid is presented in the image 4.3.

Table 4.7: Line parameters of the Urban MV benchmark distribution grid.

From bus	To bus	Resistance (Ω/km)	Reactance (Ω/km)	I_{max} (A)
1100	1101	0.203764	0.105633	620
1101	1102	0.203764	0.105633	620
1102	1103	0.062436	0.01694	440

1100	1104	0.203764	0.105633	620
1104	1105	0.203764	0.105633	620
1105	1106	0.062436	0.01694	440
1100	1107	0.203764	0.105633	620
1107	1108	0.203764	0.105633	620
1108	1109	0.062436	0.01694	440
1100	1110	0.265958	0.137819	620
1110	1111	0.265958	0.137819	620
1111	1112	0.265958	0.137819	620
1111	1113	0.066308	0.018029	440
1112	1114	0.066308	0.018029	440
1100	1115	0.074536	0.057354	805.45
1115	1116	0.074536	0.057354	805.45
1116	1117	0.074536	0.057354	805.45
1117	1118	0.074536	0.057354	805.45
1118	1119	0.074536	0.057354	805.45
1119	1120	0.074536	0.057354	805.45
1120	1121	0.074536	0.057354	805.45
1116	1122	0.054208	0.014641	440
1118	1123	0.054208	0.014641	440
1119	1124	0.054208	0.014641	440
1121	1125	0.054208	0.014641	440
1100	1126	0.074536	0.057354	805.45
1126	1127	0.074536	0.057354	805.45
1127	1128	0.074536	0.057354	805.45
1128	1129	0.074536	0.057354	805.45
1129	1130	0.074536	0.057354	805.45
1130	1131	0.074536	0.057354	805.45
1131	1132	0.074536	0.057354	805.45
1127	1133	0.054208	0.014641	440
1129	1134	0.054208	0.014641	440
1130	1135	0.054208	0.014641	440
1132	1136	0.054208	0.014641	440
1100	1137	0.091718	0.070543	805.45
1137	1138	0.091718	0.070543	805.45
1138	1139	0.091718	0.070543	805.45
1139	1140	0.091718	0.070543	805.45
1140	1141	0.091718	0.070543	805.45
1141	1142	0.091718	0.070543	805.45
1142	1143	0.091718	0.070543	805.45
1143	1144	0.091718	0.070543	805.45
1144	1145	0.091718	0.070543	805.45
1138	1146	0.057112	0.015488	440
1140	1147	0.057112	0.015488	440

1141	1148	0.057112	0.015488	440
1143	1149	0.057112	0.015488	440
1145	1150	0.057112	0.015488	440
1100	1151	0.06655	0.051183	805.45
1151	1152	0.06655	0.051183	805.45
1152	1153	0.06655	0.051183	805.45
1153	1154	0.06655	0.051183	805.45
1154	1155	0.06655	0.051183	805.45
1155	1156	0.06655	0.051183	805.45
1156	1157	0.06655	0.051183	805.45
1157	1158	0.06655	0.051183	805.45
1158	1159	0.06655	0.051183	805.45
1159	1160	0.06655	0.051183	805.45
1160	1161	0.06655	0.051183	805.45
1161	1162	0.06655	0.051183	805.45
1162	1163	0.06655	0.051183	805.45
1163	1164	0.06655	0.051183	805.45
1164	1165	0.06655	0.051183	805.45
1165	1166	0.06655	0.051183	805.45
1152	1167	0.072842	0.019844	440
1154	1168	0.072842	0.019844	440
1155	1169	0.072842	0.019844	440
1157	1170	0.072842	0.019844	440
1159	1171	0.072842	0.019844	440
1161	1172	0.072842	0.019844	440
1162	1173	0.072842	0.019844	440
1164	1174	0.072842	0.019844	440
1166	1175	0.072842	0.019844	440

Table 4.8: Transformer parameters of the Urban MV benchmark distribution grid.

From bus	**To bus**	**Rated power (MVA)**	**Voltage1 (kV)**	**Voltage2 (kV)**	**U_k (%)**	**U_r (%)**
1000	1100	90	0	12	12	0.5

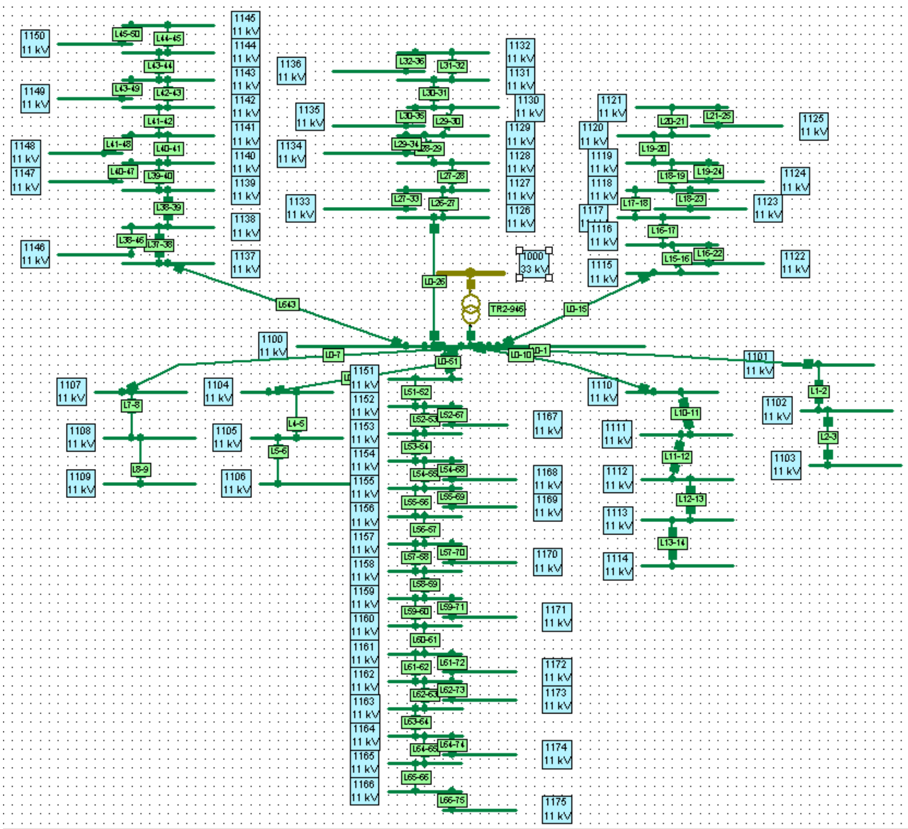

Figure 4.3: Sketch of the Urban MV benchmark distribution grid.

Chapter 5

Benchmark grids simulations

The three benchmark grids presented in the previous chapter are used to disperse the prosumers. Some households, industrial and commercial loads are dispersed onto the grid, with a high penetration of renewable units (PV, wind) but trying to be as realistic as possible. However, in some cases the amount of generation was chosen to be very large in order to obtain interesting results. One part of the household loads was chosen to be a thermal load, representing around 7% and 2% of the total amount of load in two different grids. Then the remaining large RES units are dispersed according to different strategies and locations, explained in the following chapters.

The chosen simulation period goes from 15th March until 15th June to gather high PV and wind infeed together, as well as different load configurations (from end of winter to beginning of summer). This applies to all of the simulations.

5.1 Low Voltage Microgrid: Base case

In this simulation arrangement, the benchmark distribution grid shown in Chapter 4.1 has the load demand and RES in-feed installed power capacity ratings that are detailed in Table 5.4.

The grid has three different feeders, a short feeder on the middle and two ramified feeders on the left and on the right. As this is a low voltage grid, each feeder was designed to host one kind of consumer: on the left feeder there are residential consumers, on the middle there are industries and on the right, prosumers with commercial loads. Compared to the case of the scenario of the rural MV grid, there is a bigger penetration of PV, which will lead to more frequent overvoltages and overloadings compared to

Table 5.1: Load and generation dispersion on LV benchmark microgrid.

Bus ID	Type of Prosumer	Number	Load (kW)	Generation (kW)
R11 R15 R16 R17 R18	Household with PV	10	60	65
I2	Industry with Wind PV Plant	1 1	50 0	100 350
C9 C12 C13 C14 C17 C18 C19 C21	Commercial with PV	8	120	160
C1 R16 I2	PV Plant	3	0	1050
C6 R6	Wind farm	2	0	700
C15	Wind farm	1	0	150

Table 5.2: Summary data from LV Grid base simulation case.

Energy produced by units	922.6 MWh
Energy consumed by units	159 MWh
Energy losses (lines and transformers)	39.91 MWh

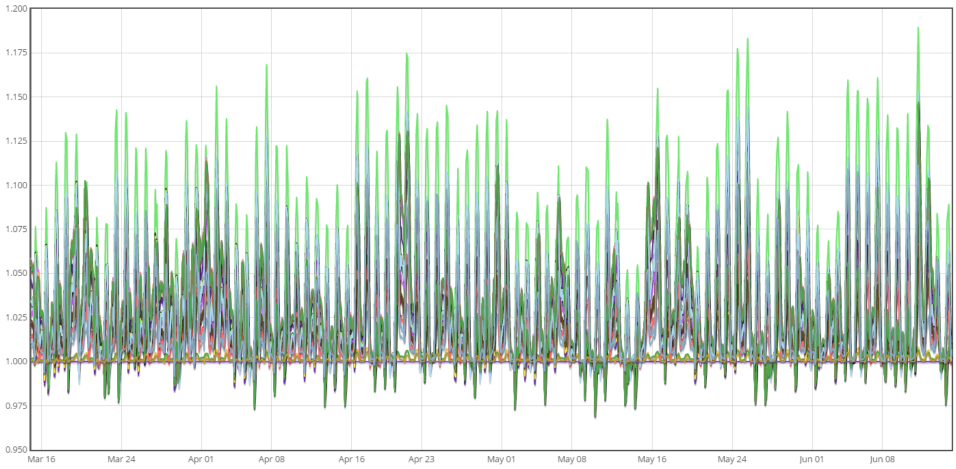

Figure 5.1: Bus voltages of the LV distribution microgrid.

wind, as it can be observed in Fig. 5.1. By comparison to the scenarios found in the next section, there is a much higher RES penetration but in this case it is not located at the very end of the feeder, which increases significantly the maximum permissible power in-feed at the considered grid node.

The total electricity consumption (load), electricity production values from RES units (e.g. available wind turbine and PV power in-feed) as well as component losses over the simulation period are also given in Table 5.2.

5.2 Rural Medium Voltage Grid: Base case

In this simulation setup, the benchmark distribution grid shown in Chapter 4.2 has the load demand and RES in-feed installed power capacity ratings that are detailed in Table 5.4.

The grid has two different feeders, a ramified feeder on the left and a shorter one on the right. On the left side, there is a bigger proportion of household loads as the right feeder it is mostly industrial. On the end buses of the left feeder, there are two wind farms with an installed capacity of 13 MW each. On the buses near the transformer there are two big loads, representing other subgrids that are not modelled in detail. Even though

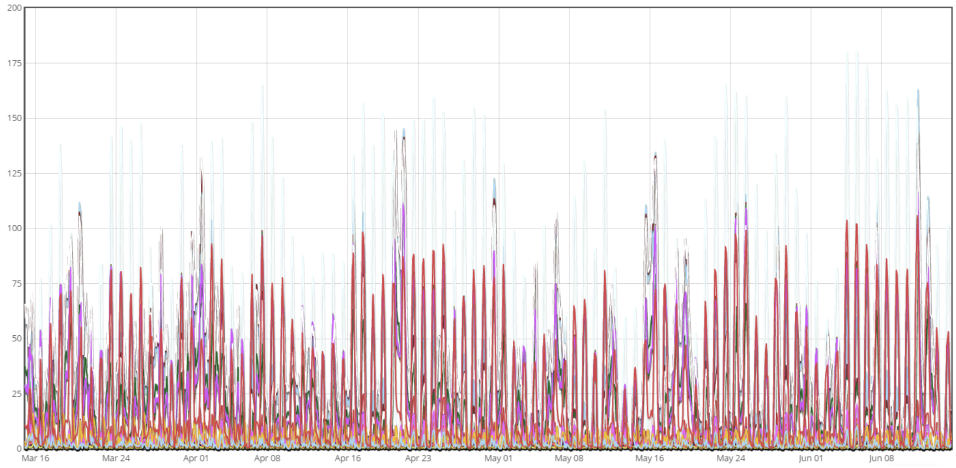

Figure 5.2: Line loadings of the LV distribution microgrid.

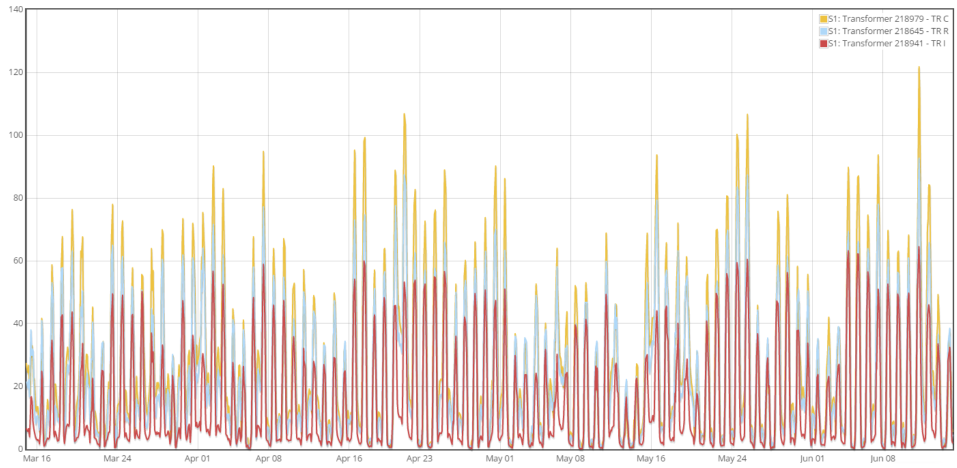

Figure 5.3: Transformer loadings of the LV distribution microgrid.

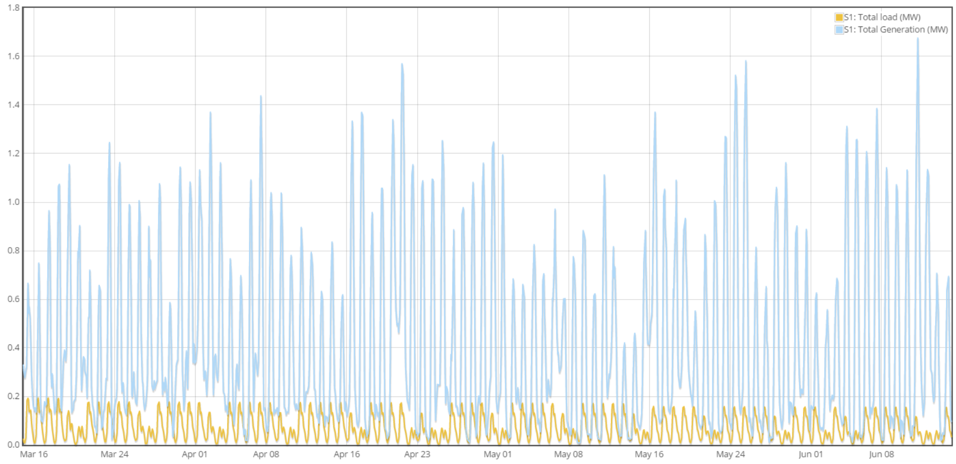

Figure 5.4: Aggregated load and generation of the LV distribution microgrid.

Table 5.3: Summary data from rural MV grid base simulation case.

Energy produced by units	11 555 MWh
Energy consumed by units	2 740 MWh
Energy losses (lines and transformers)	427.48 MWh

these are relatively large loads for the size of the grid, they will not produce any bad effects due to their proximity to the slack bus.

The total electricity consumption (load), electricity production values from RES units and lines and transformer losses over the simulation period are also given in Table 5.3.

As it can be seen in Fig. 5.5, due to several voltage violations, not all RES energy infeed can be hosted in this MV grid. However, lines and transformer loading limits are fulfilled (see Fig 5.6 and 5.7). This behaviour is motivated because the voltage rises due to the wind farms location in the grid but the amount of generation power is not so large for the lines to overload. These wind farms are located (on purpose) at the very end of the feeder, far away from the slack bus. The fact that the lines and transformers are not overloaded leaves some margin to solve the overloadings with approaches such as OLTC Transformers or reactive power control.

In the voltage plot (Fig. 5.5), two groups of buses can be found, one that remains between 1 and 0.99 per unit approximately and one that has a much more volatile voltage profile up to around 1.12 per unit. This is a clear effect of the topology of the grid and distribution of generation, as the right feeder does not have so much amount of generation and the voltage

Table 5.4: Load and generation dispersion in the MV rural benchmark distribution grid.

Bus ID	**Type of Prosumer**	**Number**	**Load (kW)**	**Generation (kW)**
416044	Household	85	510	0
416035	Household with TCL	75	600	0
416038	Household with PV	150	900	975
416056	Household with Wind	25	150	150
416029 416050 416047 416041 416139 416142	Household	60	360	0
	Household with TCL	55	440	0
	Household with PV	100	600	650
	Household with Wind	25	150	150
	Industry	18	900	0
	Industry with PV	9	450	630
	Industry with Wind	9	450	585
416044 416056	Wind Farm	2	0	26 000
416001	Subgrid	1	15 000	0
416136	Industrial subgrid	1	5 000	0

rise of the left feeder does not affect the buses on the right.

The aggregated load and generation graphics are also given in Fig. 5.8.

5.3 Urban Medium Voltage Grid: Base case

In this simulation case, this radial distribution grid shown in Chapter 4.1 has the load demand and RES in-feed installed power capacity ratings that are detailed in Table 5.6.

There is a very high infeed of RES, which will lead to frequent overvoltages and overloadings. Compared to PV power plants, the installed power of the wind farms is larger, although PV overvoltages are much more frequent due to its daily behaviour. These overvoltages are also higher in magnitude because of the location of PV sources. The total electricity consumption (load) as well as electricity production values from RES units (e.g. available wind turbine and PV power in-feed) over the simulation period are also given.

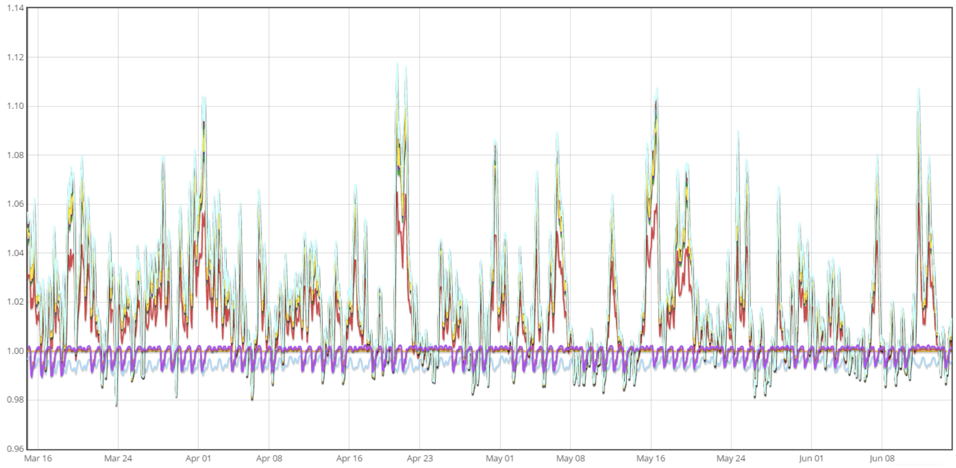

Figure 5.5: Bus voltages of the MV rural distribution grid.

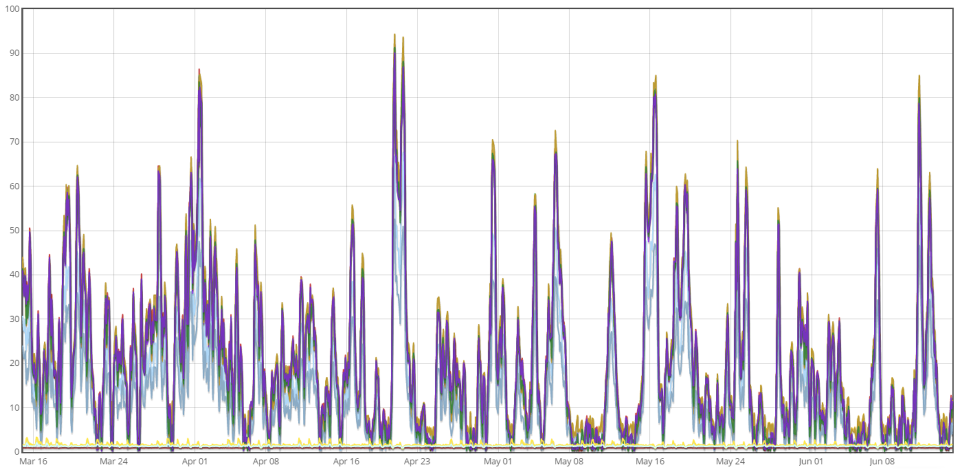

Figure 5.6: Line loadings of the MV rural distribution grid.

Table 5.5: Summary data from urban MV grid base simulation case.

Energy produced by units	76 622 MWh
Energy consumed by units	11 156 MWh
Energy losses (lines and transformers)	4 196 MWh

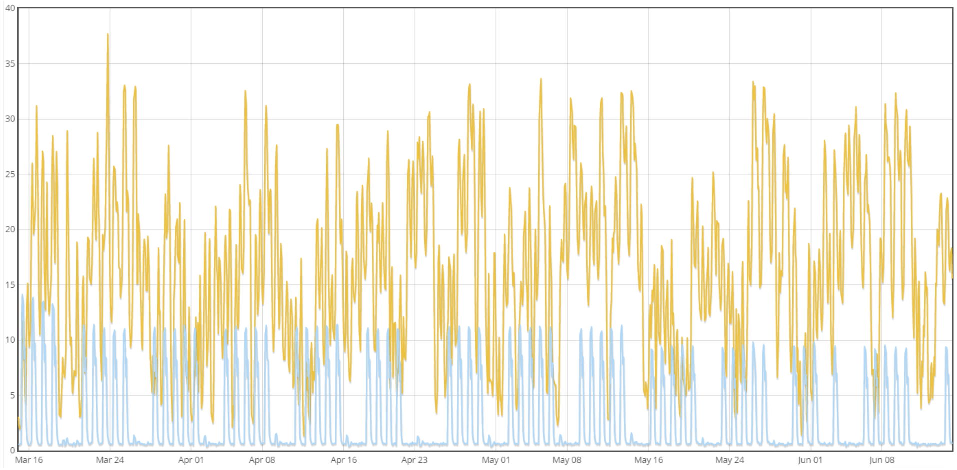

Figure 5.7: Transformer loadings of the MV rural distribution grid.

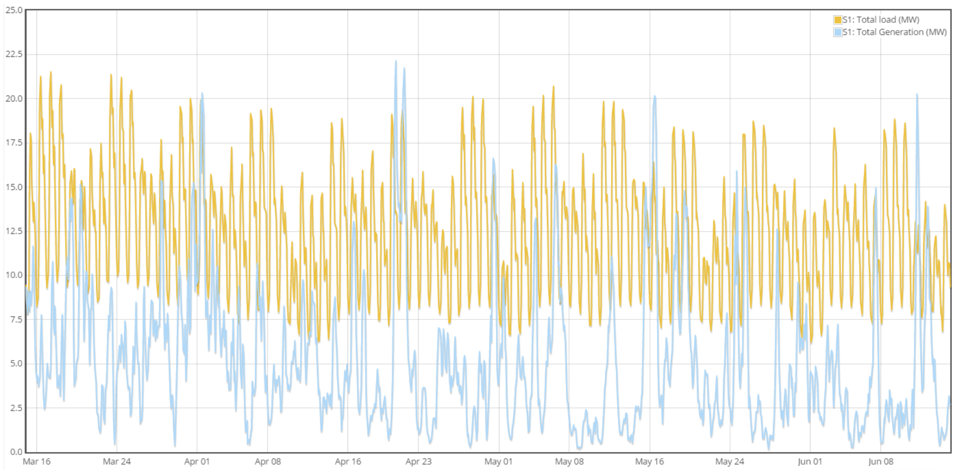

Figure 5.8: Aggregated load and generation of the MV rural distribution grid.

Table 5.6: Load and generation dispersion in urban MV distribution grid.

Bus ID	**Type of Prosumer**	**Number**	**Load (kW)**	**Generation (kW)**
23, 27, 30	Industry	18	900	0
33, 36, 39 240, 688, 691 852, 855, 875	Industry with PV	54	2 700	3 780
42, 45	Industry with Wind	9	450	65
485, 482, 506 503, 688, 691 694, 700, 843 846, 849, 852 855, 875, 858 861, 872	Household Household with TCL Household with PV	75 65 150	450 520 900	0 0 975
57, 60, 63 240, 243, 246 264	Commercial Household Household with TCL Household with PV	140 35 30 70	2 100 280 240 420	0 0 0 455
187, 190, 193 216, 219, 222	Household with Wind Commercial	120 100	720 1 500	720 0
479, 476, 473 470, 494, 491 500, 497, 622 625, 628, 631 634, 637, 640	Household with PV Industry Industry with PV	100 25 25	600 1 250 1 250	650 0 1 750
728, 731, 734 737, 740, 743 746, 749, 752 755, 758, 761 764, 767, 835 846	Household Household with TCL Household with PV Household with Wind	60 55 150 75	360 440 900 450	0 0 975 450
48, 755, 264 485, 764, 193	Wind Farm	8	0	12 0000
54, 488, 637	PV Plant	3	0	66 000

As it can be seen in Figs. 5.9, 5.10 and 5.11, due to several voltage and loadings violations, this medium-scale MV grid cannot withstand all

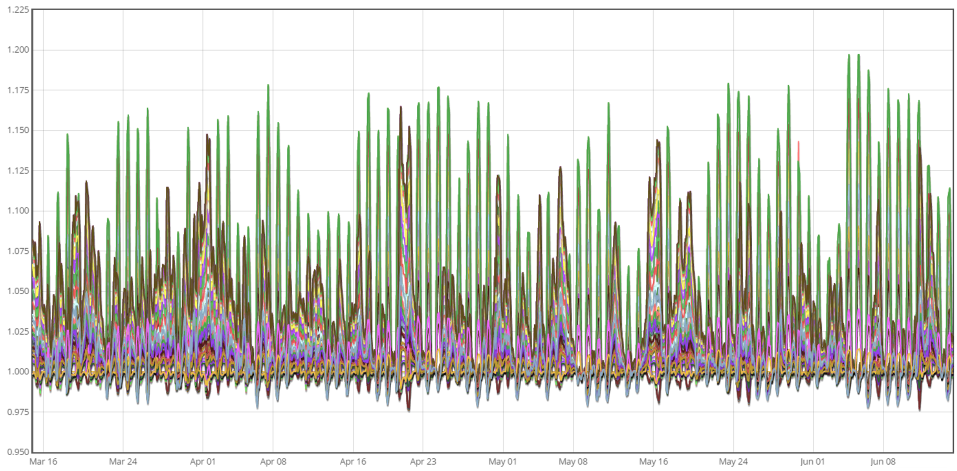

Figure 5.9: Bus voltages of the urban MV distribution grid.

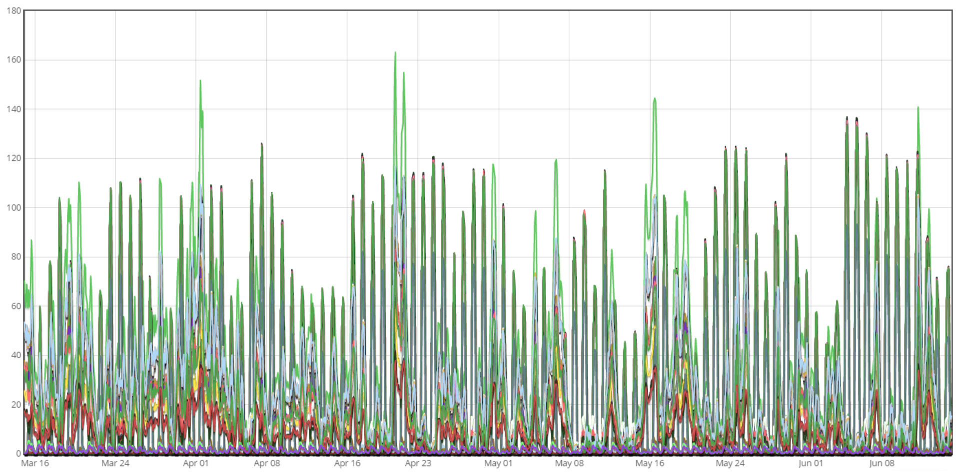

Figure 5.10: Line loadings of the urban MV distribution grid.

the energy fed by RES within the required limits. In this case, voltage violations and lines overloadings are coinciding and both are caused by the large amount of generation.

In the voltage plot (Fig. 5.9), buses affected by wind or PV power can be clearly distinguished. However, there is a small interrelation between feeders and voltages, due to the topology and parameterization of the grid. This behaviour is shown in Fig. 5.13, where the voltage of the bus 700 changes when a battery is activated in another feeder.

The aggregated load and generation graphics are also given in Fig. 5.12.

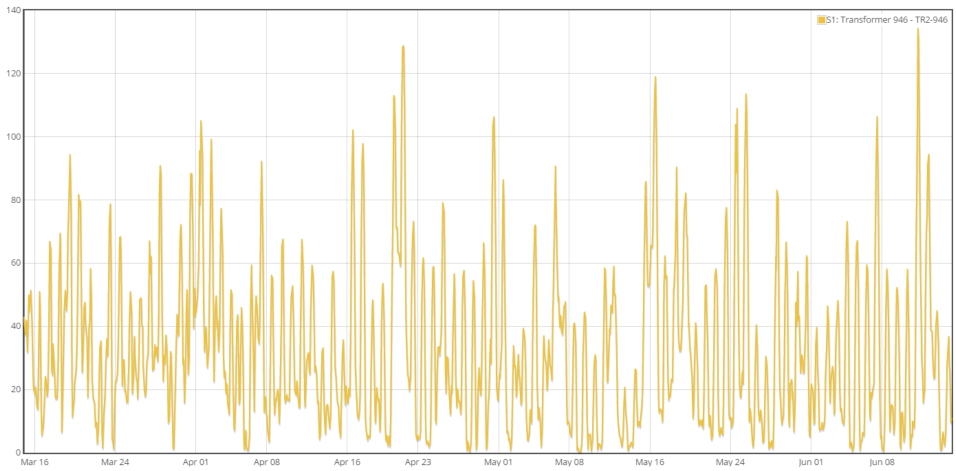

Figure 5.11: Transformer loadings of the urban MV distribution grid.

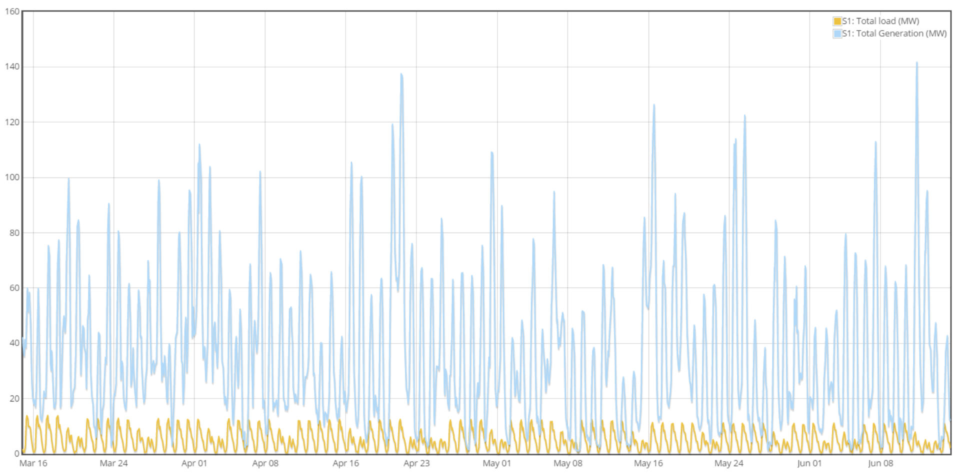

Figure 5.12: Aggregated load and generation of the urban MV distribution grid.

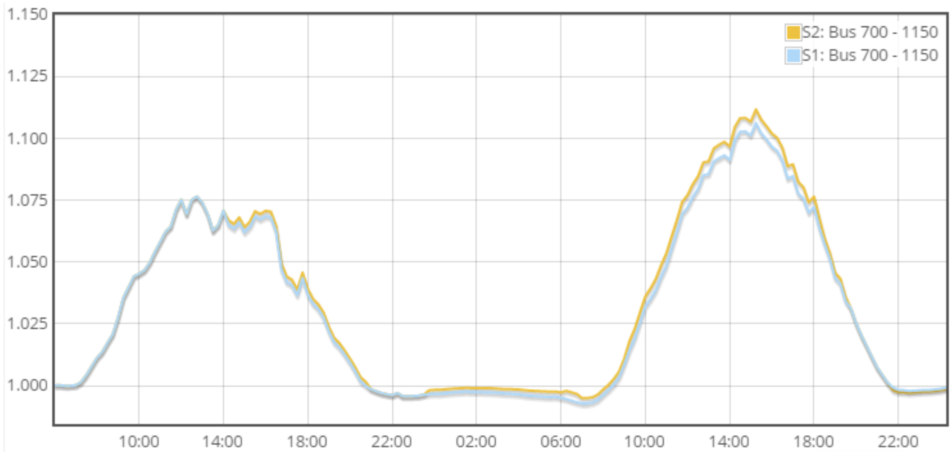

Figure 5.13: Bus 700 voltage base case (blue) and with charging storage in a different feeder (yellow).

Chapter 6

Operation strategies

This chapters includes four sections: technical requirements, energy curtailment, battery control and other control strategies. The latter sections present an overview of different operation strategies and and provide a basis for selecting suitable strategies to be used in the following chapter.

6.1 Technical requirements in distribution grids

Voltage lies within permissible range of ±10%

Maintaining the appropriate voltage in all parts of the distribution grid is a crucial task of a Distribution System Operator (DSO). The principal voltage quality requirements are set forth in the EN 50160 industry standard [12]. The most relevant requirement for the performance evaluation in this project is requirement to keep the voltage within +/- 10% of the nominal value (i.e. in the corridor from 0.9 to 1.1 per unit). Consequently, the performance of every SmartGrid approach on every grid is evaluated by its capability to keep the voltage within this permissible corridor.

Grid element loadings within permissible range

The loading level of a distribution line or transformer (here referred to as grid element) denotes the ratio of the current flowing through the line and the stipulated maximum current. Thus, it needs to be kept under 100% for grid security reasons. Overloads will trigger protection devices in order to avoid thermal damage to the grid element, and consequently lead to power outages for customers. The maximum current in a grid element is also a function of the duration of the loading level: due to the thermal inertia of the element, it is permissible to overload it for a short duration. We will try to dimension the control strategies so as to keep the loadings in our simulations under the lower and more conservative maximum bound.

6.2 Energy curtailment

As it was stated before, curtailment is the easiest strategy to solve grid overvoltages and overloadings. In this work, the same curtailment percentage was applied to all units regardless of their contribution to the grid problem. As the violation of the technical requirements is caused by energy generation, just curtailing excess generation power will make the requirements to be fulfilled. The curtailment control strategies are introduced in DPG.sim as predefined rules: if the predefined conditions are fulfilled, i.e. the permissible range is exceeded, then curtailment is applied. Two different ways of applying curtailment can be distinguished (Fig. 6.1):

- Curtail a percentage of the current infeed when there is a problem on the grid. This can lead to the undesired effect of very fast voltage drops and rises, as shown in the yellow curve in Fig. 6.2. This is because the predefined magnitude of the power curtailment is based on the worst case scenario with maximum PV infeed and minimum load conditions, so it will lead to more curtailed energy than needed, with its compensation cost. This can be solved by applying several curtailment rules with different magnitudes depending on the intensity of the voltage violation but much easier is the following approach.
- Curtailing all the generation power that exceeds a defined fraction of the installed capacity. This avoids the implementation of several control rules and leads to a much flatter curtailment. There is still a voltage drop some days, as the amount of installed capacity that the grid can host also depends on the load conditions and the power to be curtailed is based on the worst case scenario. The behaviour of this control strategy is shown in blue in both Fig. 6.1 and 6.2.

The second option is definitely better in terms of ease of use and operational behaviour so it will be be implemented in the curtailment scenarios.

6.3 Battery control

Batteries are a way to make use of the energy that the grid cannot host providing energy to the grid when the energy costs are higher, for instance, because there is less RES infeed. The batteries simulated in this study are operated such that they will not discharge under 10% capacity and will not

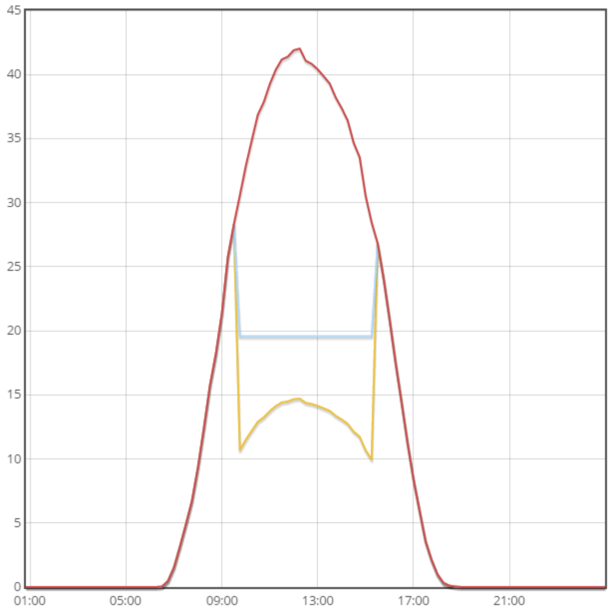

Figure 6.1: Generation without curtailment (red), with percentage infeed (yellow) and with capacity curtailment (blue).

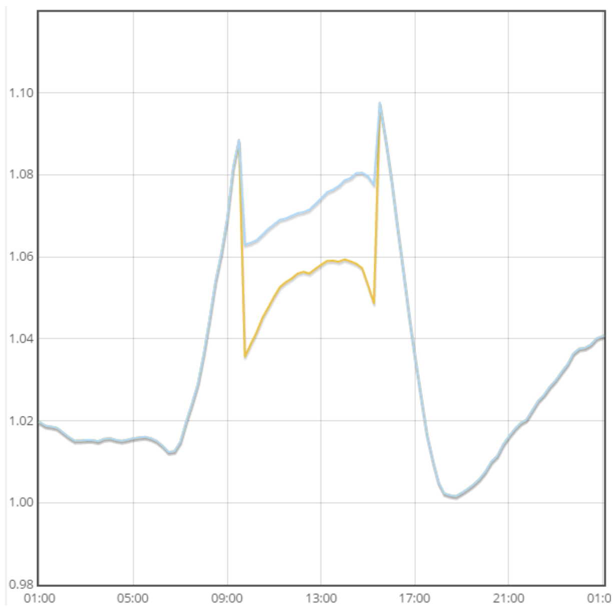

Figure 6.2: Bus voltage with infeed percentage curtailed (yellow) and with excess infeed curtailed (blue).

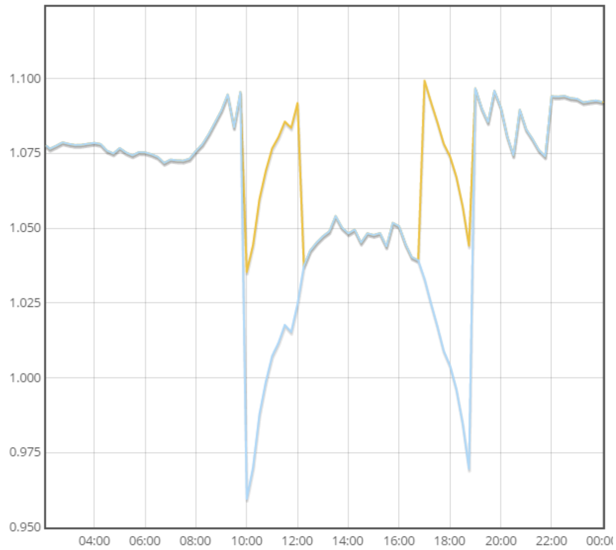

Figure 6.3: Bus voltage with a one only charging rule or two.

charge over 90% capacity. The round-trip efficiency is 0.903. In the following chapters, the effect of the differences between concentrated storage, i.e. a big battery, and dispersed storage, i.e. one battery for each PV and wind unit, is studied. As for the control strategy, it is not possible to design a rule to charge the surplus energy of a PV/wind unit and, as there is no communication between the units and the batteries, the batteries do not know how much RES infeed there is at each time step. The following two ways will then be the options to consider (represented in Fig. 6.3):

- The implementation of a fixed power amount to charge the battery when there is an overvoltage or overloading and regardless of its magnitude. It is a simple strategy but it can lead to exactly the same large and sudden voltage drop seen in the previous section with energy curtailment. This effect is shown in the blue curve in Fig. 6.3).

- Another approach is to define several rules to charge the battery according the voltage violation intensity (yellow curve in fig. 6.3). The design of this strategy can be more time-consuming if trying to make it very precise, i.e. a lot of voltage steps with their respective battery charging and discharging powers.

The effect of the latter approach is better in terms of voltage drop magnitude and it will be the way to go for the simulations in the next chapter.

6.4 Other control strategies

In the following chapter, further SmartGrid strategies are used: reactive power control and OLTC transformer. The reactive power control strategy is based on reactive power injection to decrease node voltages and the OLTC transformer enables stepped voltage regulation of the secondary side of the transformer (and therefore of the connected feeder).

As these operation strategies are simpler than batteries or curtailment, remaining details of the operation are given in the following chapter, within the sections where these SmartGrid approaches are used.

Chapter 7

Simulation results

7.1 LV Grid: Curtailment

The first and easiest option to solve grid problems is curtailment. In this case, a different curtailment strategy has been defined on each feeder, according to the specific setup of each. Once an overloading or overvoltage is detected in the residential feeder (left feeder in Fig. 4.1), RES capacity will be limited to 30% of its full capacity although the actual generation will still depend on the infeed of solar/wind energy. The industrial feeder is limited to 60% of its full capacity and the commercial one (right feeder) to 40% capacity.

With these rules, the grid can now operate under normal conditions, as can be observed in the voltage and loadings plots 7.1, 7.2 and 7.3.

The Fig. 7.5 shows the generation power in each time step and can easily be compared with Fig. 5.4. It can be concluded that more than 450 kW of generation power can never be hosted although sometimes even more capacity (up to around 700 kW as shown in Fig. 7.4) is curtailed, because it depends on the load conditions. Curtailed energy and energy losses are included in Table 7.1.

Table 7.1: Summary data from LV Grid scenario with energy curtailment.

Curtailed energy	66.7 MWh (7.22%)
Energy losses (lines and transformers)	29.88 MWh (-25.1%)

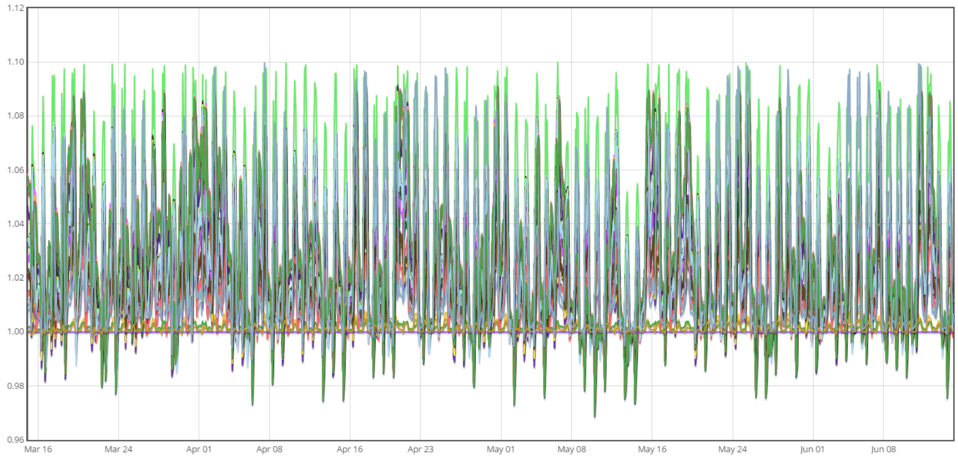

Figure 7.1: Bus voltages of the LV distribution microgrid with energy curtailment.

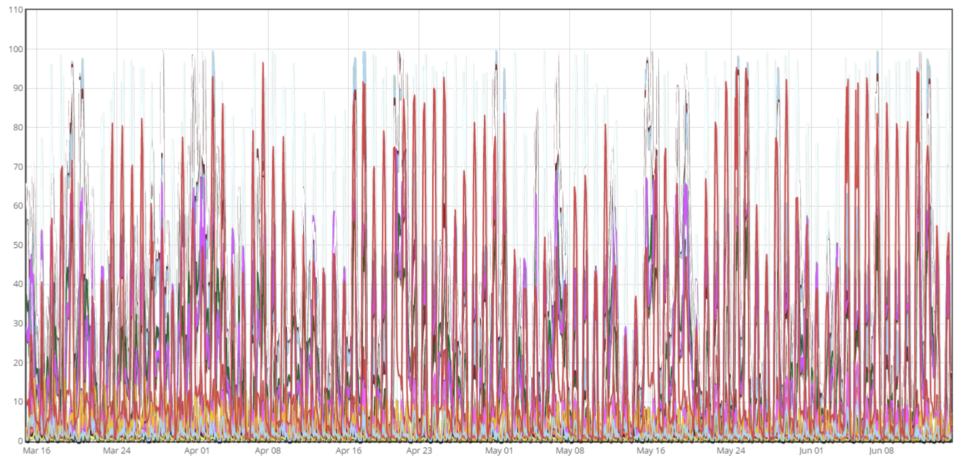

Figure 7.2: Line loadings of the LV distribution microgrid with energy curtailment.

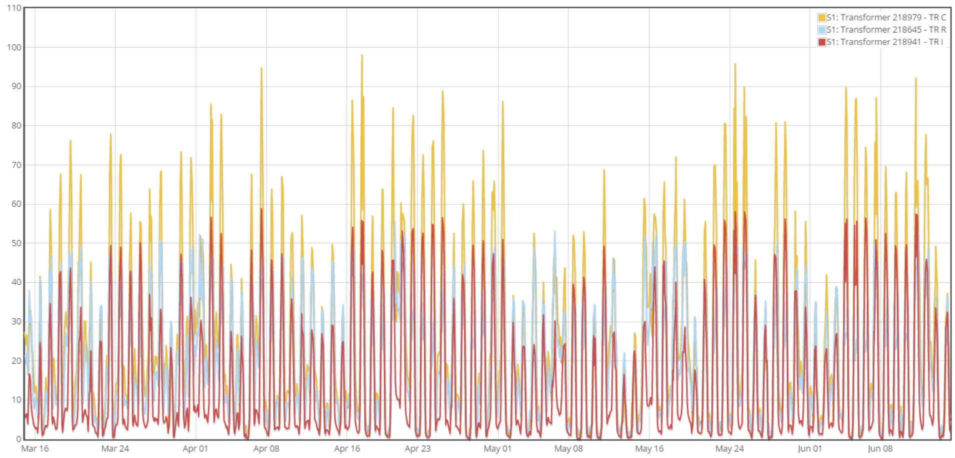

Figure 7.3: Transformer loadings of the LV distribution microgrid with energy curtailment.

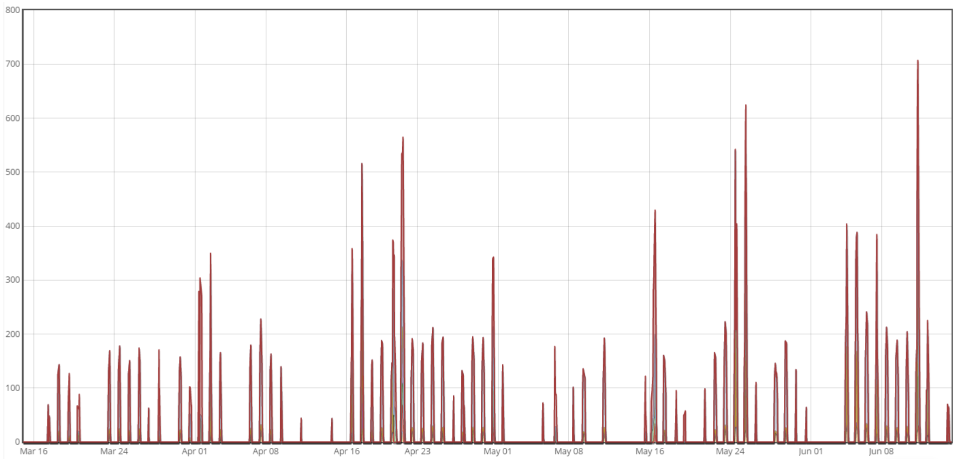

Figure 7.4: Curtailed power of the LV distribution microgrid with energy curtailment (in kW).

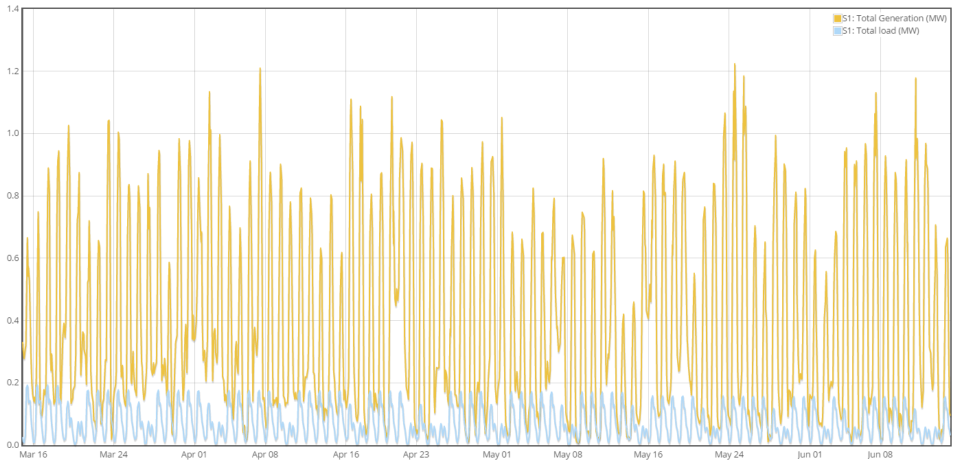

Figure 7.5: Aggregated generation of the LV distribution microgrid with energy curtailment.

7.2 LV Microgrid: Concentrated Storage

In order to increase the grid hosting capacity of RES, three batteries have been installed. The initial idea was to increase the hosting capacity with just one big battery to be able to clearly see the difference between concentrated and dispersed storage. The idea was tested and ruled out, as the grid has three almost independent voltage profiles, corresponding to each of the three feeders. The effect of the activation a battery on the left feeder is not observable in the voltage profile of the right feeder (the order of magnitude is around 10^{-5} per unit).

Another issue to address was the location of the battery. Although the planned location (for greater convenience of the grid operator) was as close to the transformers as possible, this idea proved to be technically inefficient and had to be discarded: the effect of the batteries on the voltage profile was very little and there were still a lot of overloaded lines. For the same amount of power, the closer to the transformer and slack bus, the less the voltage drop or rise. The second location to try was one that was neither close to the transformer nor behind a service connection line, so it was still a convenient location (service connection lines are weaker lines that connect the buses where the prosumers are located (in ramifications) to the main part of the feeder). This worked for the right feeder because the biggest generation plant was already before a service connection line, which are weaker. However, on the left feeder, where the most problematic power plant was located behind a service connection line, the new location of the storage definitely led to a significant voltage reduction but could not resolve all the overloading problems. Particularly, the lines between the PV plants

Table 7.2: Battery R parametrization in LV grid with concentrated storage.

Battery R (400 kW - 5 200 kWh)
Power 37,5% if (1.10<V<1.16) or (100%<L<130%)
Power 75% if (V>1.16) or (130%<L<160%)
Power 100% if (L>160%)

Table 7.3: Battery I parametrization in LV grid with concentrated storage.

Battery I (100kW - 550kWh)
Power 100% if V>1.10 or L>100%

Table 7.4: Battery C parametrization in LV grid with concentrated storage.

Battery C (250kW - 3 750kWh)
Power 40% if 1.10<V<1.14 or 100%<L<130%
Power 100% if V>1.14 or L>130%

and the battery were still overloaded as the excess flow was still going from the first to the latter.

Finally, placing the batteries together with the power plants with higher installed capacity yielded good results. The parametrization of the battery and the rules appear in Tables 7.2, 7.3, 7.4. The battery discharging starts when the voltage is under 1.075 and the lower the voltage the higher the discharging power.

The technical requirements were fulfilled and none of the lines had to be upgraded as it had been necessary in a conventional grid upgrade. The simulation results are detailed in Fig. 7.7, 7.8, 7.9 and 7.10 and line and transformer losses were reduced by 13% (5.19 MWh). However, storage losses must also be considered and these are 9.06 MWh over the simulation period. There is one single overloading that can be seen in Fig. 7.8, due to insufficient battery capacity (one of them is full at that moment). In any case, the results show that this overloading is only 2% for a short period of time and although it does not fulfill the technical requirements, it would not trigger the protections (the conservative line rating was used) so it is considered acceptable. This last conclusion is one of the advantages offered by time-series simulation instead of worst-case snapshot simulations. Fig. 7.6 shows how the voltages over 1.10 are no longer present and how the voltages under 1.02 are pushed to the 1.05-1.08 region, as the battery discharges when the voltage level decreases.

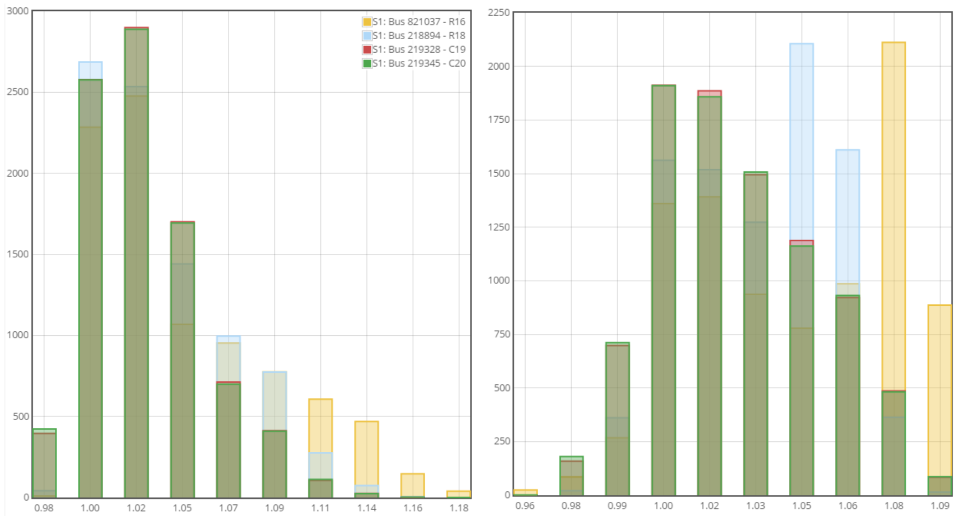

Figure 7.6: Voltages histogram of the LV distribution microgrid base case (left) and with concentrated storage (right).

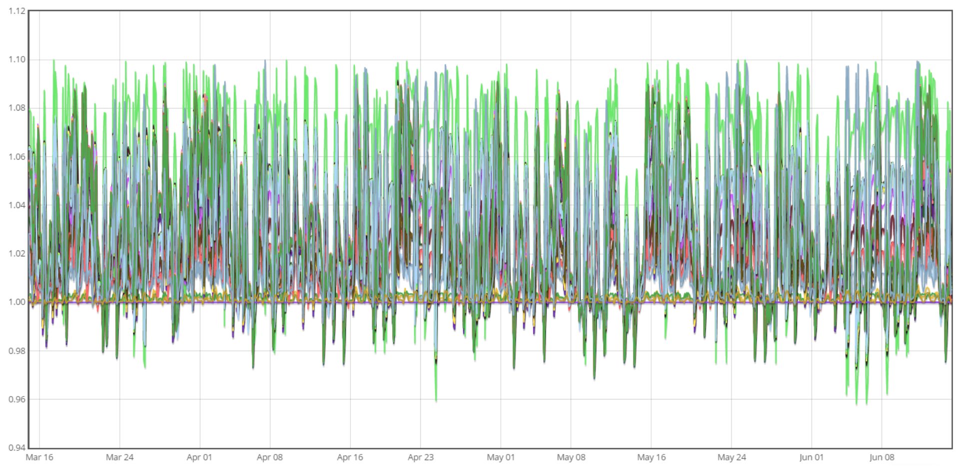

Figure 7.7: Bus voltages of the LV distribution microgrid with concentrated storage.

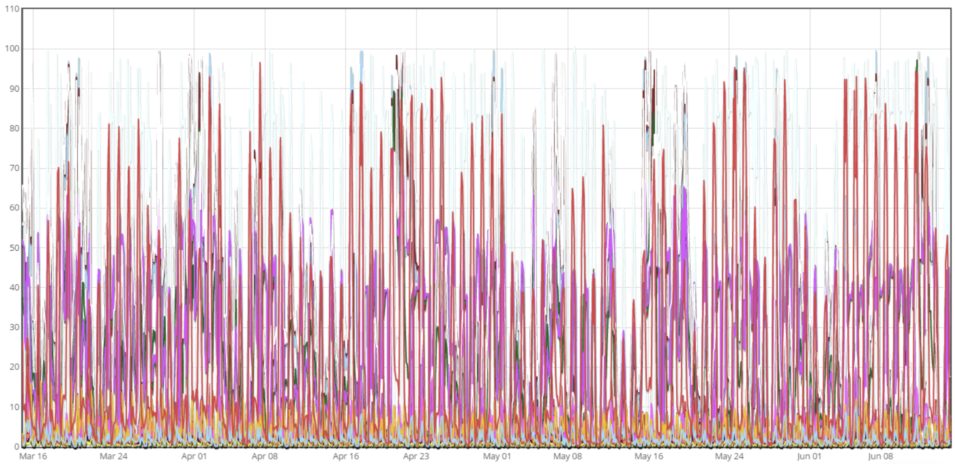

Figure 7.8: Line loadings of the LV distribution microgrid with concentrated storage.

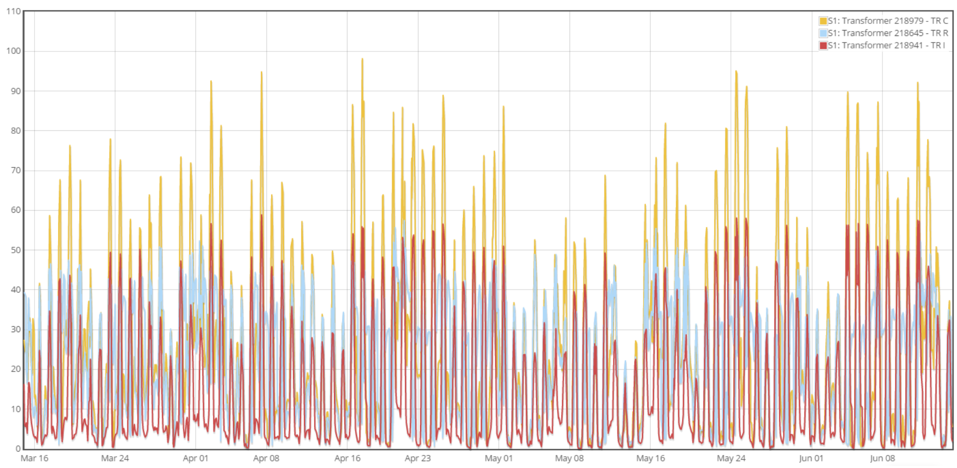

Figure 7.9: Transformer loadings of the LV distribution grid with concentrated storage.

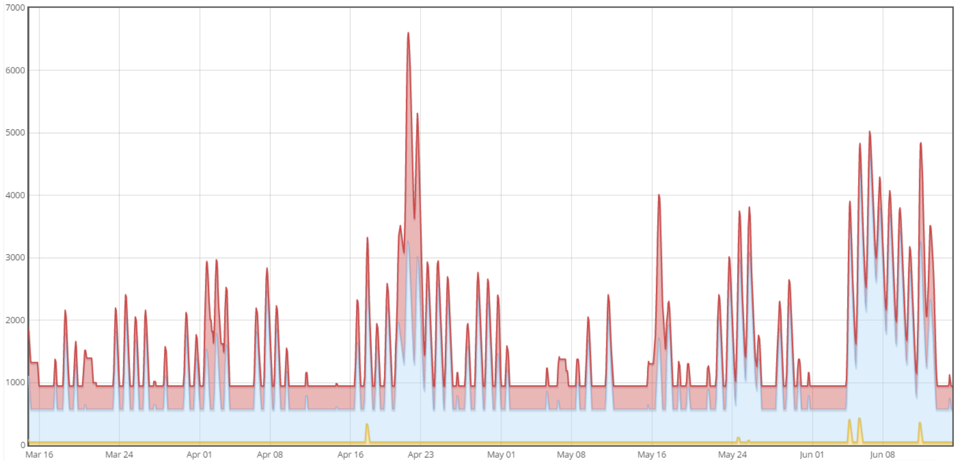

Figure 7.10: Batteries' stored energy on the LV distribution grid scenario with concentrated storage (in kWh).

In Fig. 7.11, the red curve represents the energy stored in the battery in the commercial feeder whereas the blue curve represents the energy stored in the battery in the residential feeder. The red battery has to be dimensioned in a way that it can charge for 2 consecutive days, as seen around 23th April. This happens because the overvoltages in this feeder are mostly affected by a wind farm, that can randomly produce large energy amounts for several consecutive days (opposed to what happens with PV), so this has to be taken into account for battery sizing. However, although the blue battery is mostly charging photovoltaics energy, the location of the battery does not allow to completely discharge it overnight, as it would be expected for more efficient sizing. However, the location of this battery in this bus (behind a weak line) is constrained, because otherwise the lines between the PV plant and the battery are overloaded.

7.3 LV Microgrid: Dispersed Storage

In contrast to the previous approach, one battery was installed within each prosumer that had either a PV panel or a wind unit, as well as within the power plants. Although more batteries could in principle allow for a more specific control, the controllers were set in the same way: one different behaviour for each feeder, whenever a overvoltage/overloading is detected there. The decision is adopted for ease of implementation, comparison purposes, and the fact that there will not be detrimental interaction between controllers due to the effects of activation/deactivation of batteries in the same feeder. The grid operation criteria were fulfilled as follows in

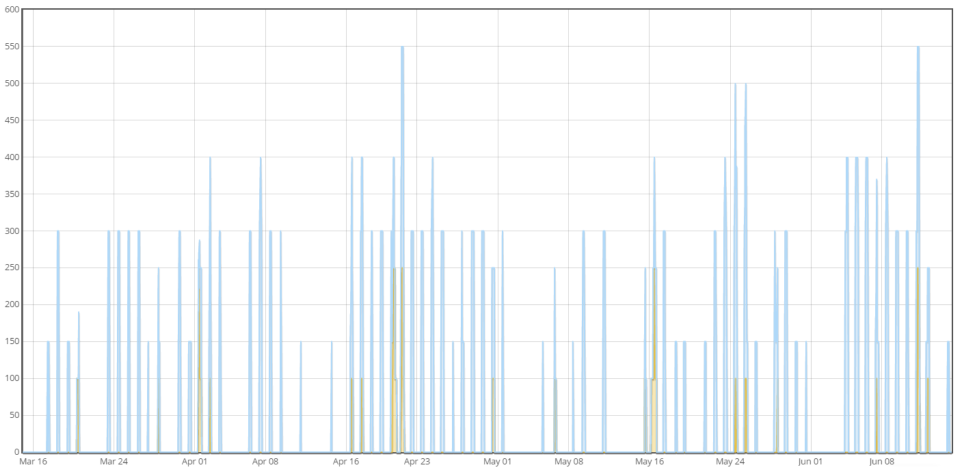

Figure 7.11: Batteries' charging power on the LV distribution grid scenario with concentrated storage (in kW).

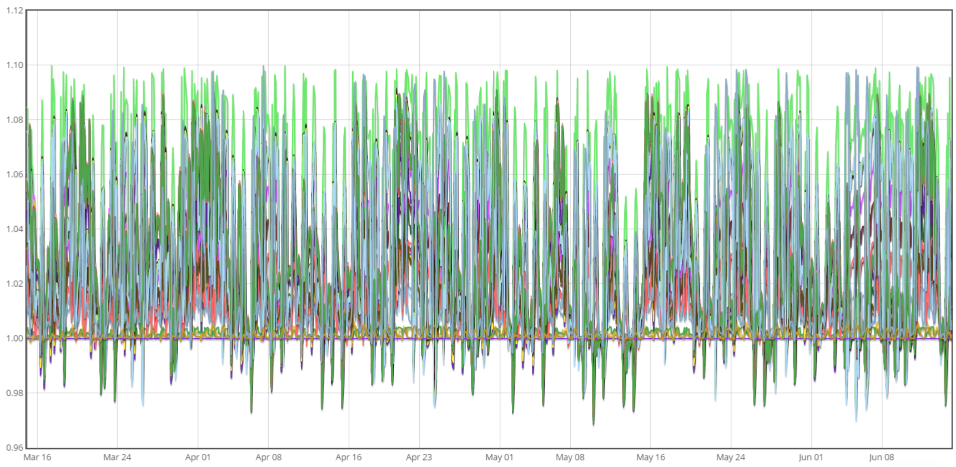

Figure 7.12: Bus voltages of the LV distribution microgrid with dispersed storage.

Fig. 7.12, 7.13, 7.14 and 7.16 and grid losses increased 5.75 MWh, due to storage losses.

7.4 LV Microgrid: Strategy comparison

Table 7.5 shows the difference between the three SmartGrid approaches to solve the LV grid scenario and how much energy can be saved with the installation of storage. The energy losses in each scenario can be compared with the initial grid losses (39.91 MWh). Table 7.6 extends the comparison

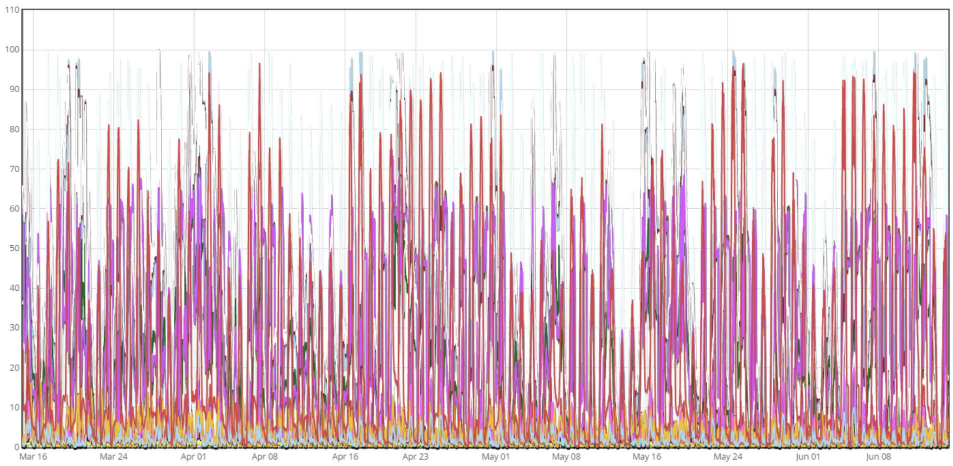

Figure 7.13: Line loadings of the LV distribution microgrid with dispersed storage.

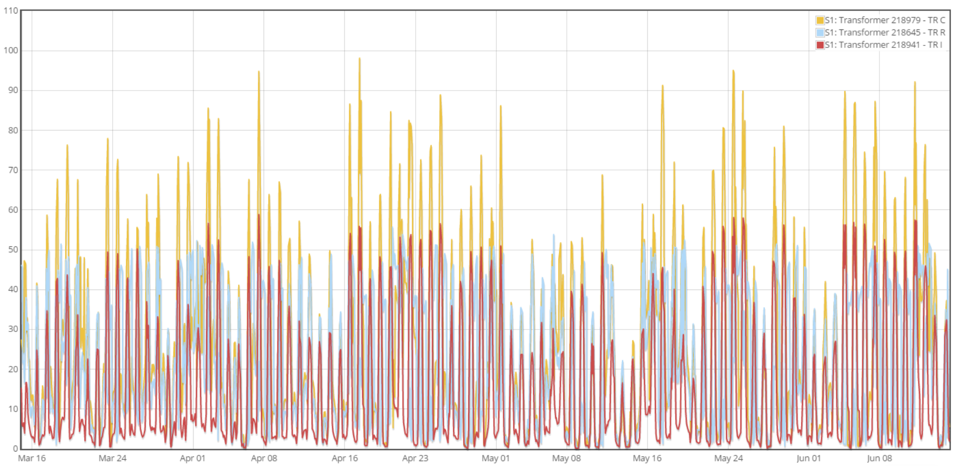

Figure 7.14: Transformer loadings of the LV distribution grid with dispersed storage.

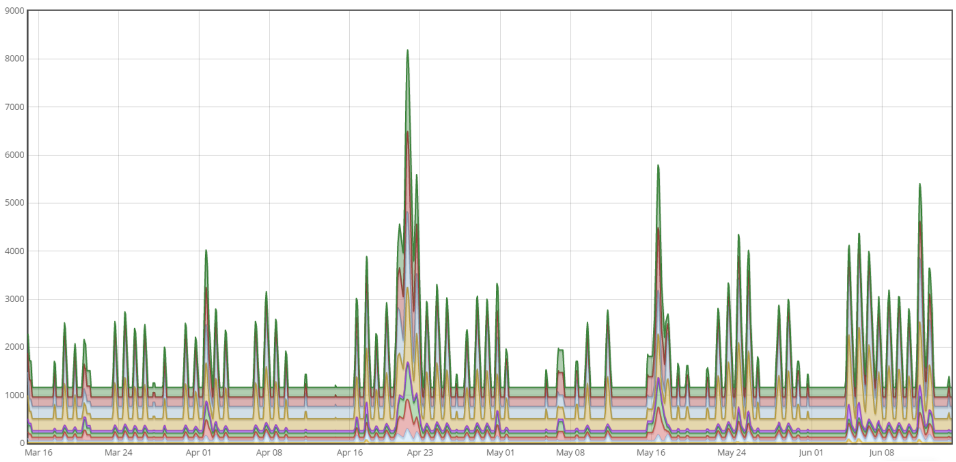

Figure 7.15: Batteries' stored energy of the LV distribution grid scenario with dispersed storage (in kWh).

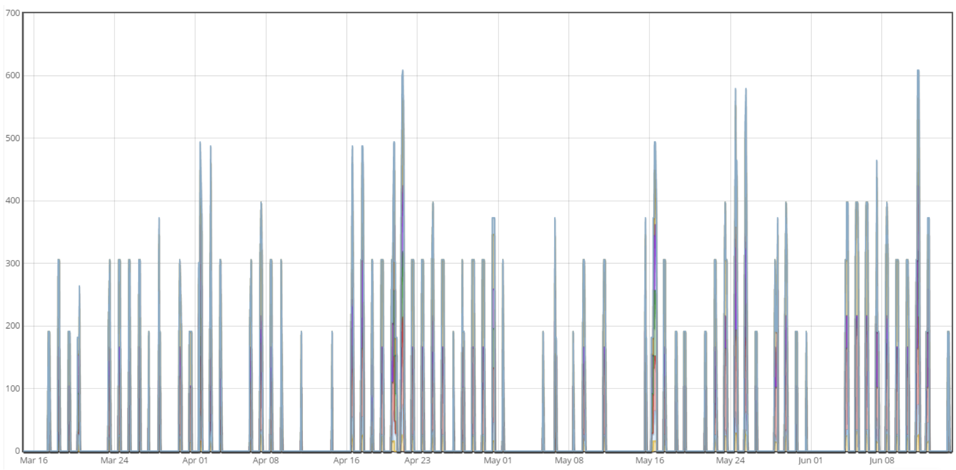

Figure 7.16: Batteries' charging power of the LV distribution grid scenario with dispersed storage (in kW).

between the two storage cases. Although the total losses in both cases are quite similar, there are some differences as far as battery capacity is concerned: random energy infeed from wind units and battery locations behind weak lines that do not allow the batteries to completely discharge overnight make the biggest difference in battery sizing. The comparison of battery sizing is summarised in Table 7.6.

Table 7.5: Losses comparison in LV scenarios.

	Curtailment	**Concentrated Storage**	**Dispersed Storage**
Curtailed energy	66.67 MWh	-	-
Line and transformer losses	29.98 MWh	34.72 MWh	35.15 MWh
Storage losses	-	10.64 MWh	9.06 MWh
Total energy losses	96.65 MWh	45.36 MWh	44.21 MWh

Table 7.6: Battery charging power and needed capacity in LV scenarios.

	Concentrated Storage	**Dispersed Storage**
Feeder R Power	400 kW	400 kW
Feeder R Capacity	4 600 kWh	3 500 kWh
Feeder C Power	250 kW	300 kW
Feeder C Capacity	3 400 kWh	4 750 kWh

7.5 Rural MV Grid: Curtailment

The control strategy implemented in this scenario was to curtail 40% of generation capacity whenever the permissible range of voltage or loadings is surpassed. Curtailment fractions are applied to each unit individually so it does not mean that 40% aggregated power is curtailed. This control rule leads to complete fulfillment of the grid operation requirements, as can bee observed in Figs. 7.17, 7.18 and 7.19.

Fig. 7.20 shows the generation power in each time step, and Fig. 7.21 shows aggregated load and generation. Both can easily be compared with the energy generation in the base scenario (Fig. 5.8). It can be concluded that more than 2 500 kW of generation capacity cannot ever be hosted (the generation power peak is around 20 MW instead of 22.5 MW). However, the curtailed energy peak is close to 6 MW, so in some cases up only 16.5 MW can be hosted under specified technical requirements.

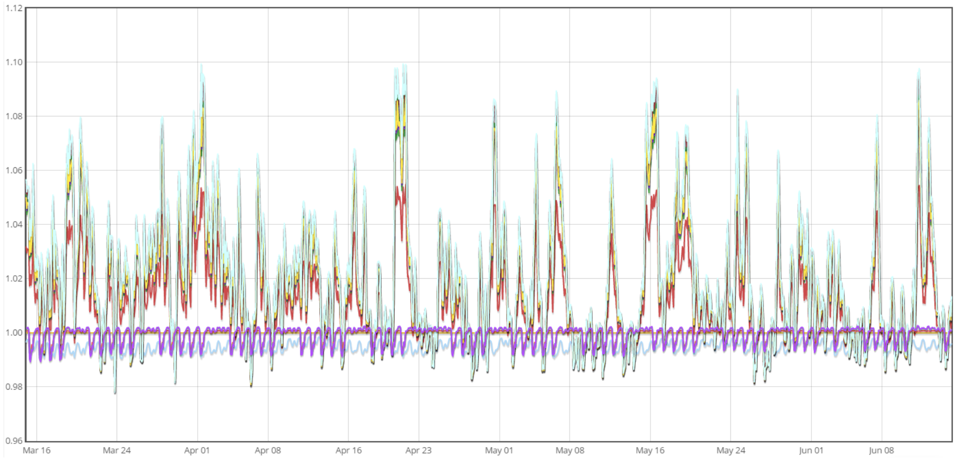

Figure 7.17: Bus voltages of the rural MV distribution grid with energy curtailment.

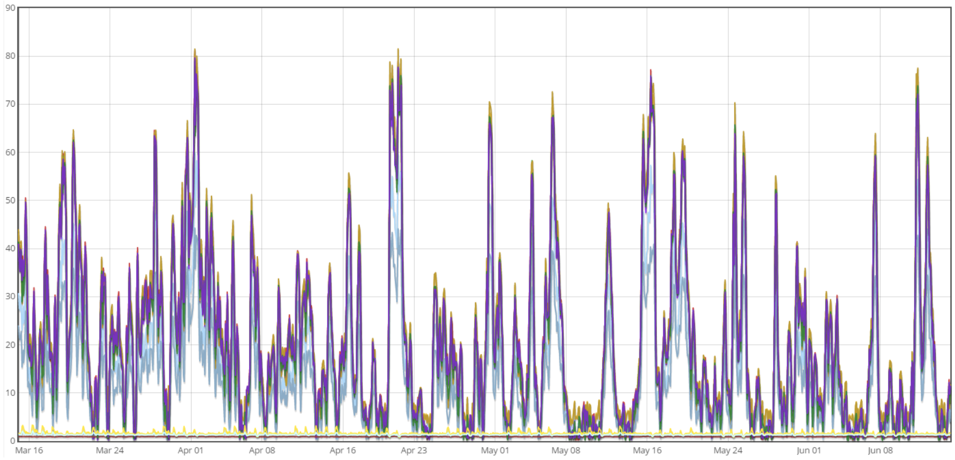

Figure 7.18: Line loadings of the rural MV distribution grid with energy curtailment.

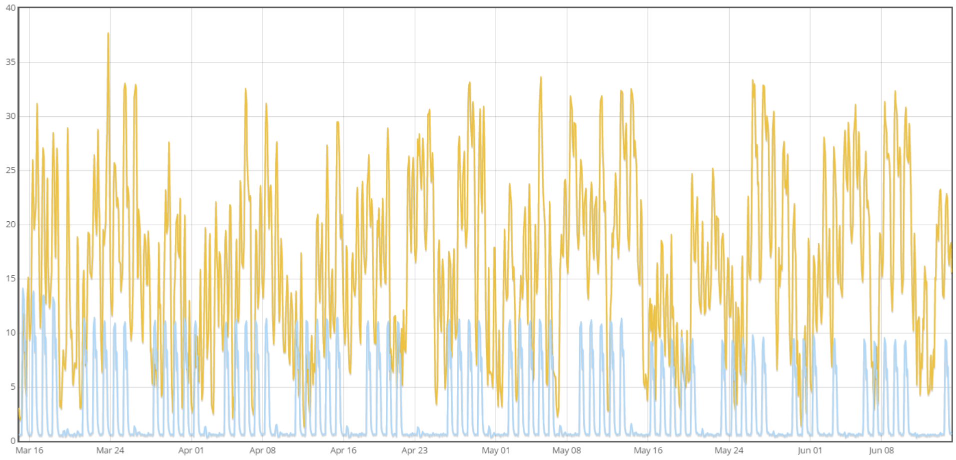

Figure 7.19: Transformer loadings of the rural MV distribution grid with energy curtailment.

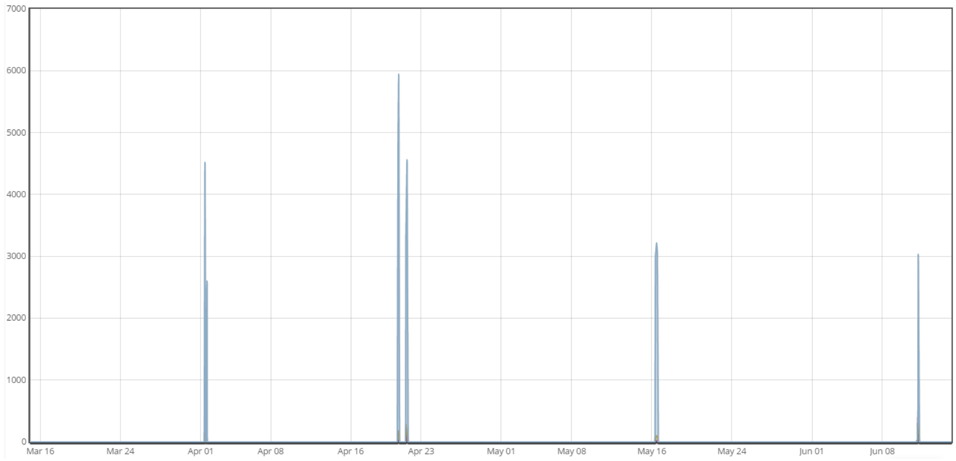

Figure 7.20: Curtailed power of the rural MV distribution microgrid with energy curtailment.

Table 7.7: Summary data from MV rural grid with energy curtailment.

Curtailed energy	73 MWh (0.63%)
Energy losses (lines and transformers)	12.77 MWh (-2.9%)

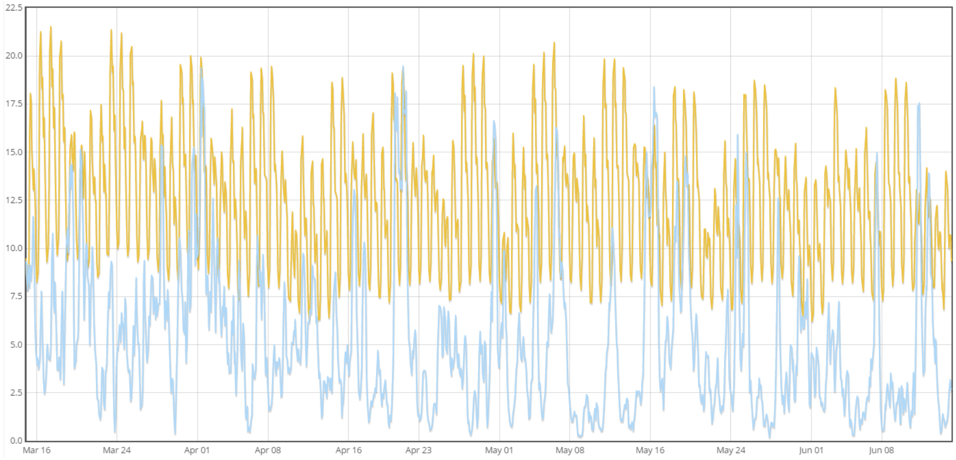

Figure 7.21: Aggregated load and generation of the rural MV distribution grid with energy curtailment (in MW).

7.6 Rural MV Grid: On Load Tap Changer Transformer

One further approach for this grid is to change the transformer of the left feeder to an OLTC transformer. The parametrization in this scenario is a transformer with 5 taps of 1% voltage with a dead band of 10%, i.e. the voltage can be between 0.9 and 1.1 without the transformer intervention. The transformer will change the tap position twice as can be seen in the voltage plot (Fig. 7.22) and the line with highest loading increases its loading by 1-1.5% on time steps with high loadings. Fig. 7.25 shows the increase of line loading due to OLTC transformer which will increase the lines and transformers losses by 9.27 MWh (2,1%)

7.7 Rural MV Grid: Reactive power control

Another strategy that yields similar results to the OLTC transformer is the production of capacitive reactive power to lower the voltages. Both wind farms at the end of the grid are substituted with two wind farms with the same installed capacity but with a capacitative cos(phi) of 0.99. Only these wind farms with their specific location will have extra production of reactive

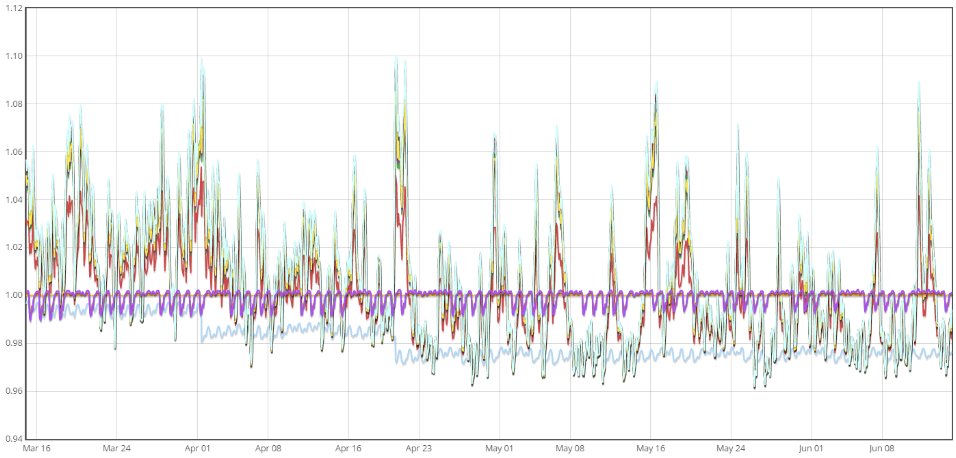

Figure 7.22: Bus voltages of the rural MV distribution grid with OLTC transformer.

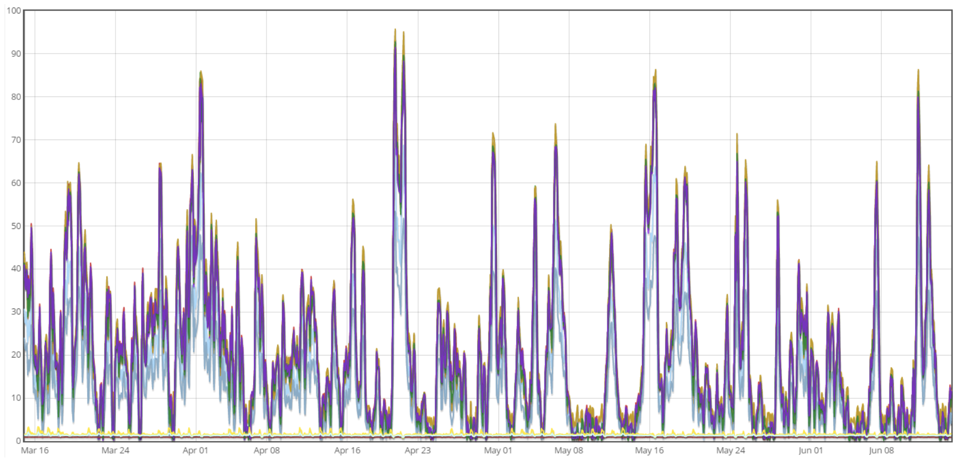

Figure 7.23: Line loadings of the rural MV distribution grid with OLTC transformer.

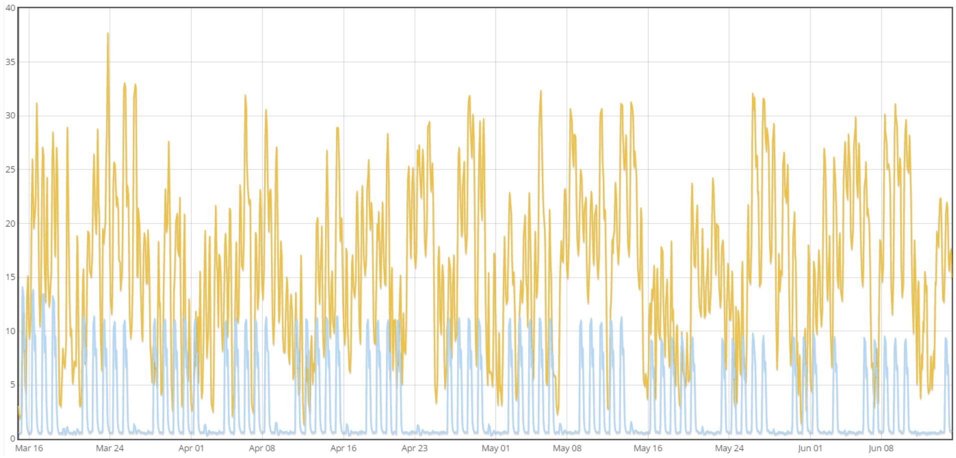

Figure 7.24: Transformer loadings of the rural MV distribution grid with OLTC transformer.

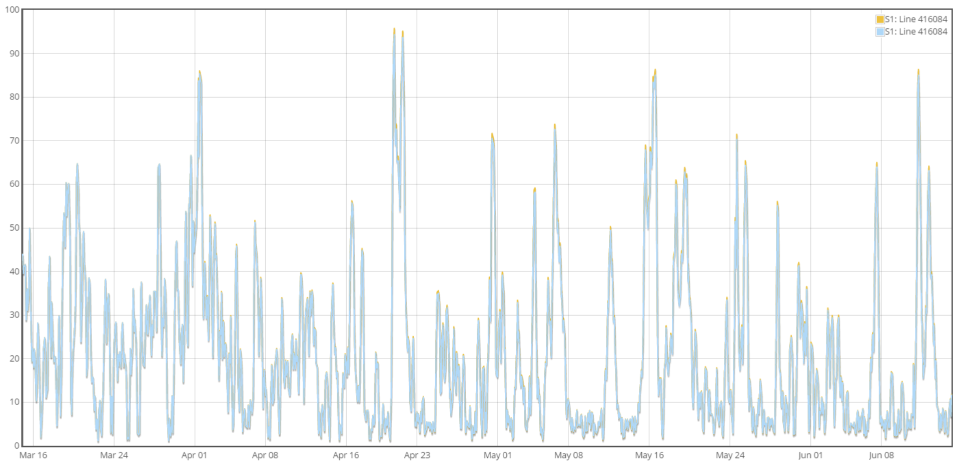

Figure 7.25: Line loading of the rural MV distribution grid with original transofrmer and OLTC transformer.

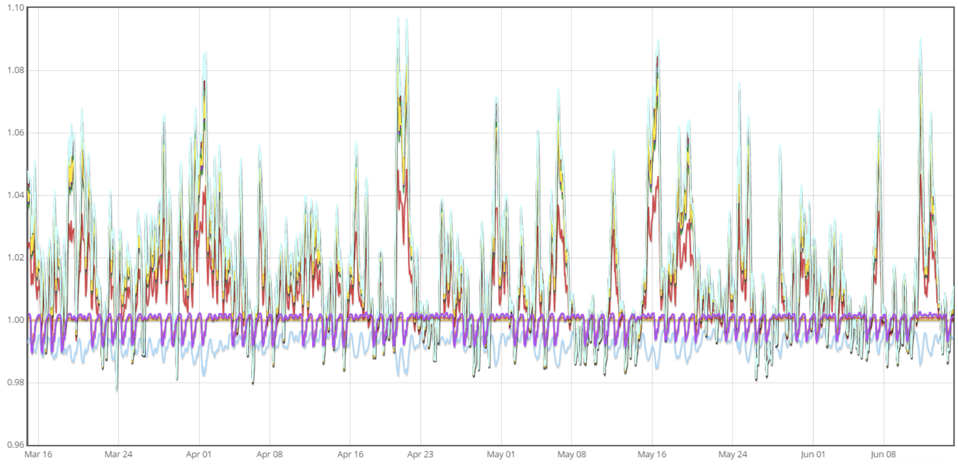

Figure 7.26: Bus voltages of the rural MV distribution grid with reactive power control.

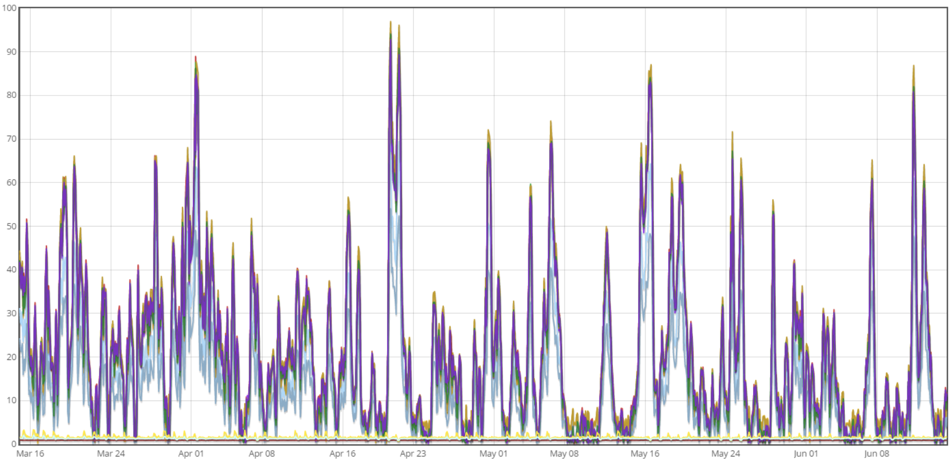

Figure 7.27: Line loadings of the rural MV distribution grid with reactive power control.

power and this will lead to the results shown in the following graphics. The increase in line loadings is shown in Fig. 7.29 and leads to an increase of 9.83 MWh (2,2%) in component losses.

7.8 Rural MV Grid: Strategy comparison

Table 7.8 presents some differences between the implemented approaches. Total energy losses can be compared with the base case losses of the rural MV grid (440.2 MWh). The reactive power control approach leads to

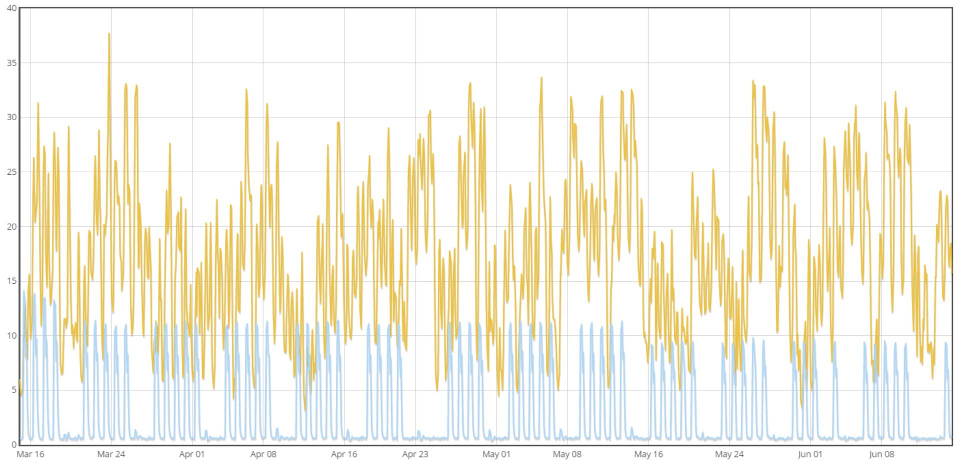

Figure 7.28: Transformer loadings of the rural MV distribution grid with reactive power control.

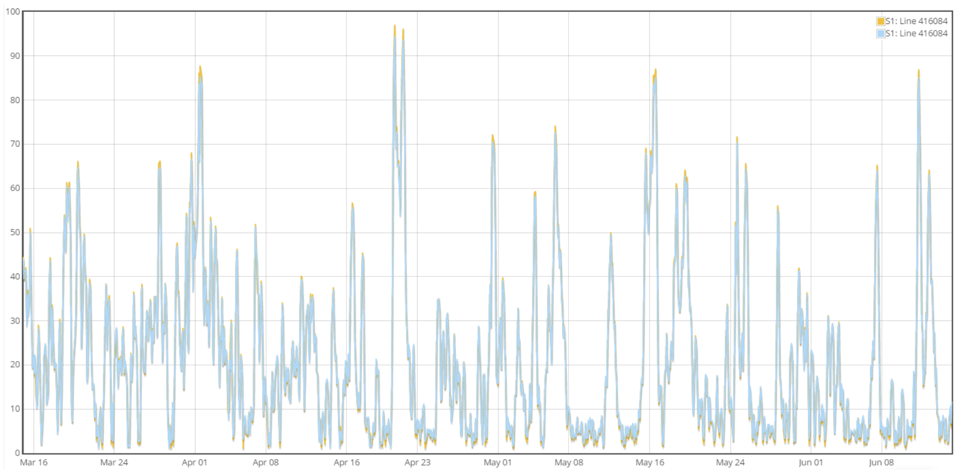

Figure 7.29: Line loadings of the rural MV distribution grid with and without reactive power control.

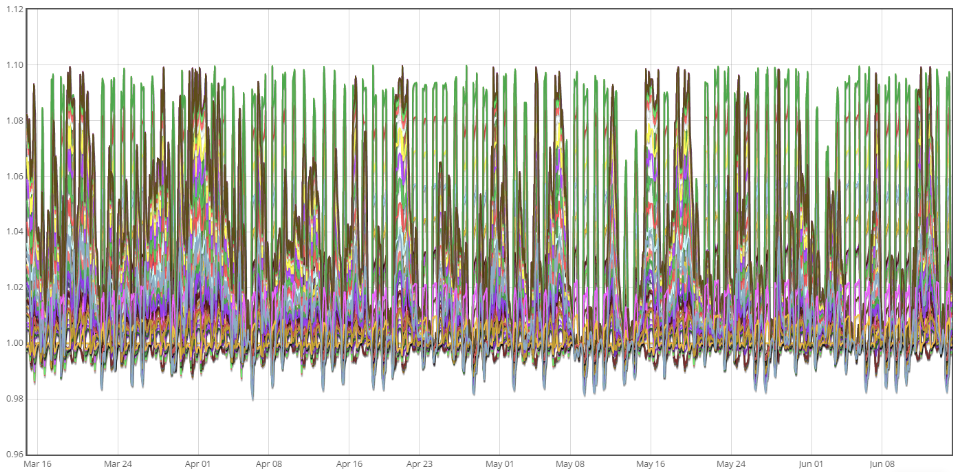

Figure 7.30: Bus voltages of the urban MV distribution grid with energy curtailment.

slightly higher losses, especially due to additional transformer losses (compared with the scenario with the OLTC transformer). The application of a more complex reactive power control, such a characteristic curve, would imply to only produce reactive power when the wind power in-feed is large and therefore reduce component losses.

Table 7.8: Losses comparison in rural MV scenarios

	Curtailment	**Tap Changer**	**Reactive Power**
Curtailed energy	73 MWh	-	-
Grid losses	427.5 MWh	449.5 MWh	450.1 MWh
Total energy losses	500.5 MWh	449.5 MWh	450.1 MWh

7.9 Urban MV Grid: Curtailment

The control strategy implemented in this scenario was to curtail 60% of the generation capacity of every unit when there is an overvoltage or a component overloading. It was implemented as the only strategy because the action of curtailing in one individual feeder of this grid has also an effect in the other feeders, so it was much easier to design one controller rule only. The strategy leads to complete fulfillment of the grid operation requirements, as can be observed in Figs. 7.30, 7.31 and 7.32.

Fig. 7.33 shows the generation power over the 3 months and is equal

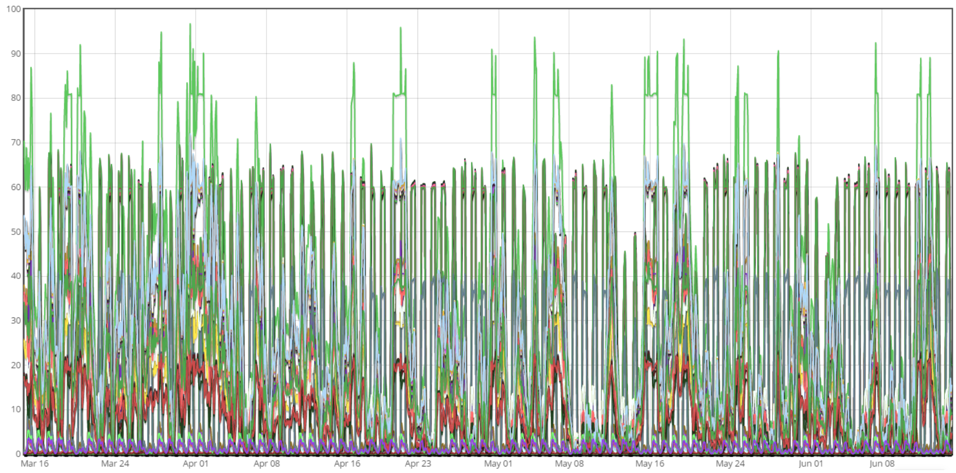

Figure 7.31: Line loadings of the urban MV distribution grid with energy curtailment.

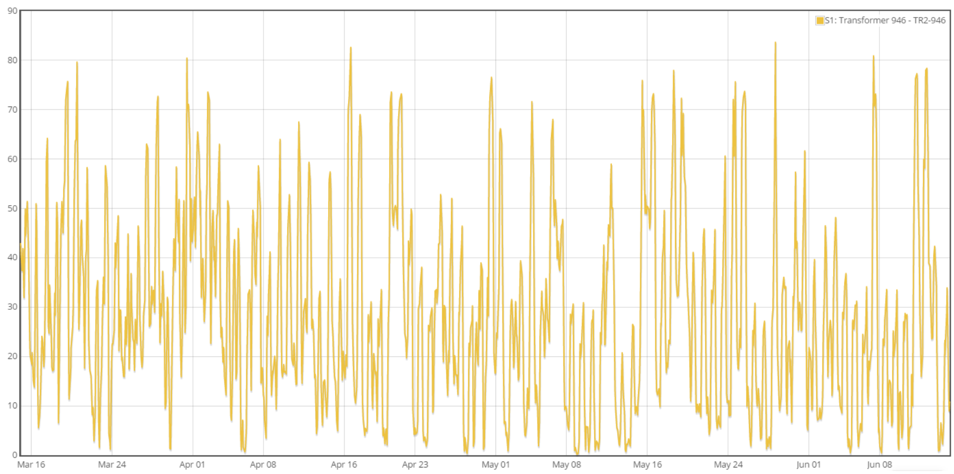

Figure 7.32: Transformer loadings of the urban MV distribution grid with energy curtailment.

Table 7.9: Summary data from MV rural grid with energy curtailment.

Curtailed energy	6 879 MWh (8.98%)
Energy losses (lines and transformers)	1 501 MWh (-35.8%)

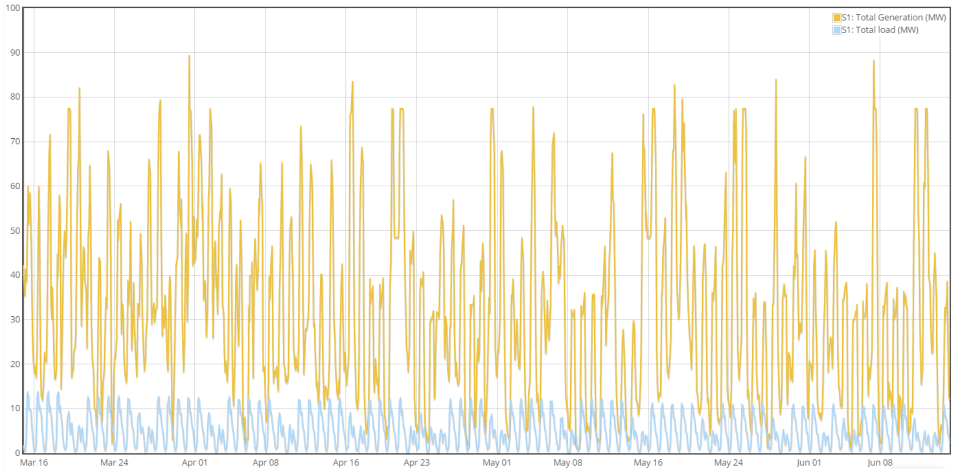

Figure 7.33: Aggregated load and generation of the urban MV distribution grid with energy curtailment.

to the graphic of the base case if the curtailment power is subtracted. It can be seen that more than 50 MW are curtailed, what in terms of energy over the 3 months simulation period means 6 879 MWh. The summary data of the simulation case is presented in Table 7.9, where the curtailed energy percentage refers to the total produced energy (76 622 MWh) and the losses percentage to the base case losses (4 196 MWh).

7.10 Urban MV Microgrid: Storage

The technical requirements were almost fulfilled as shown in Figs. 7.34, 7.35, 7.36 and 7.37 and the grid losses increased 239 MWh (5.7%) due to storage losses. There is a little overloading due to a full battery but as it is not supposed to trigger the protections, it is still considered a valid result. Fig. 7.35 shows that to fulfill the technical requirements, most of the individual feeders must be under 70% loading, which means that the voltage limit imposes a more stringent requirements on this system than the line limits. To install a tap changing transformer or a reactive power control strategy in combination with a smaller storage might be a better approach, as the installation of batteries has led to up to a 11 MW, a 20 MW and 32 MW battery.

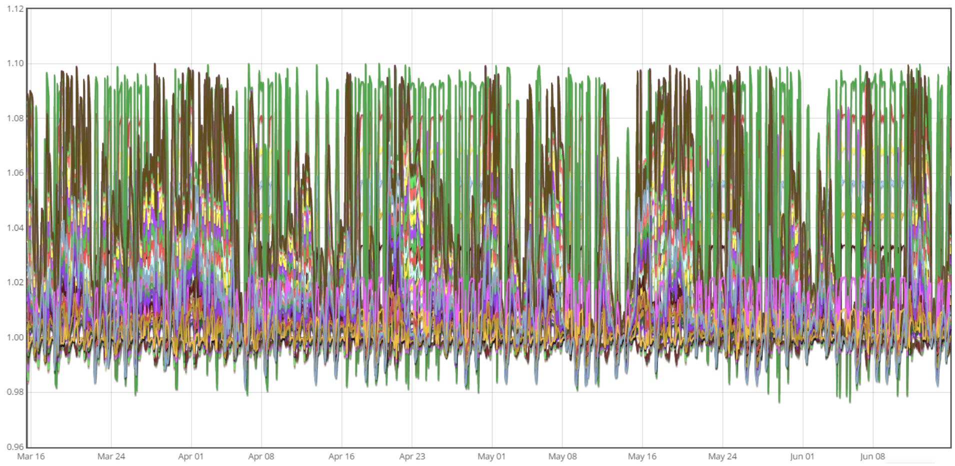

Figure 7.34: Bus voltages of the urban MV distribution grid with storage.

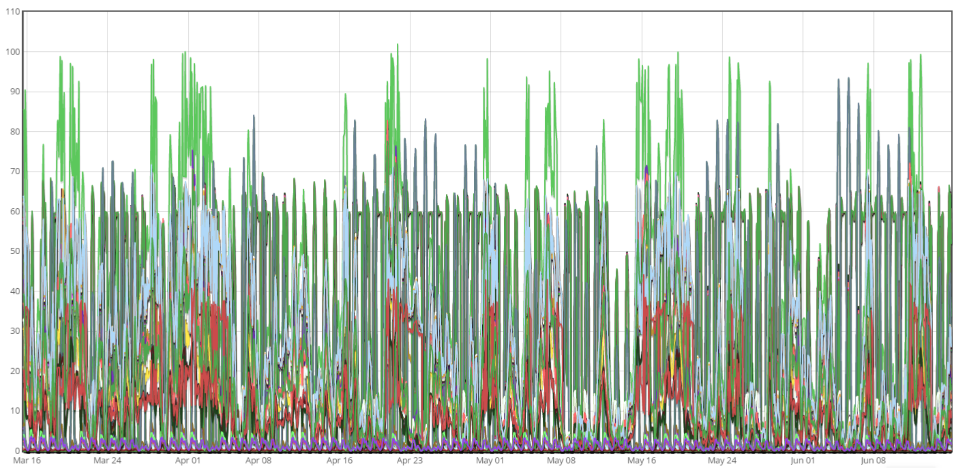

Figure 7.35: Line loadings of the urban MV distribution grid with storage.

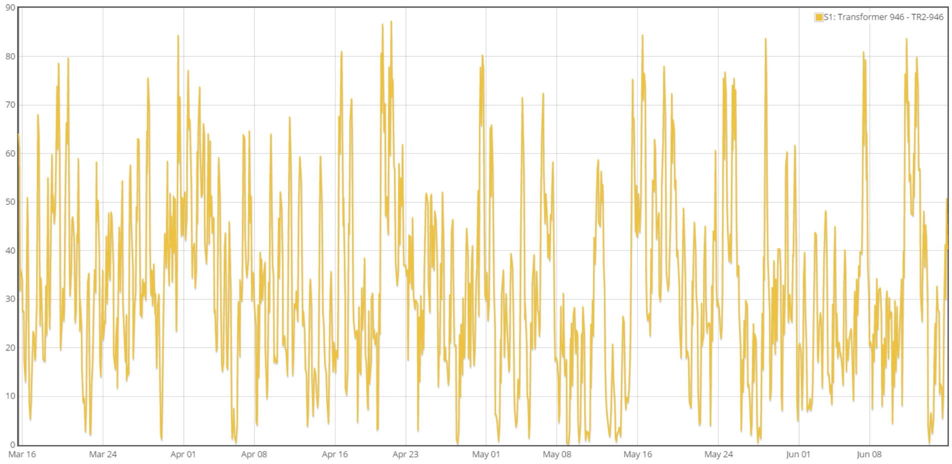

Figure 7.36: Transformer loadings of the urban MV distribution grid with storage.

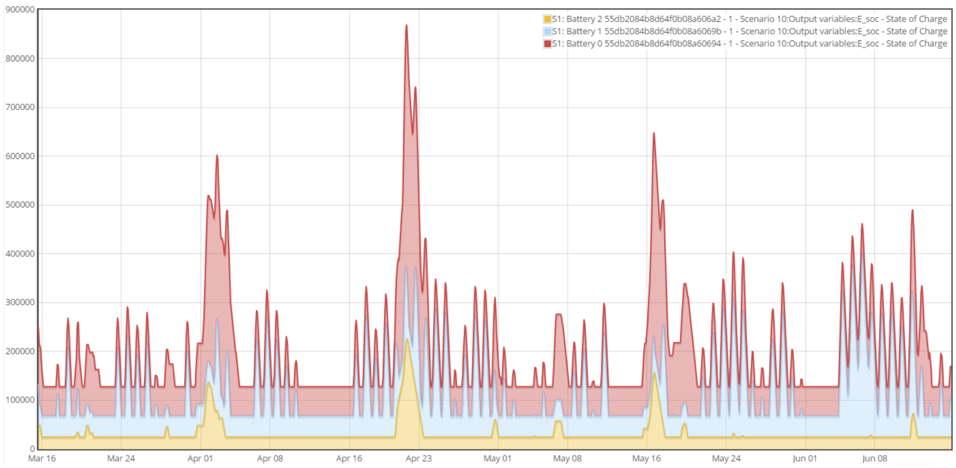

Figure 7.37: Batteries' stored energy of the urban MV distribution grid with storage (in KWh).

7.11 Urban MV Microgrid: Strategy comparison

Table 7.10 allows to compare how much energy can be saved thanks to the storage approach. The total energy losses can be contrasted with the grid losses of the base case (4 196 MWh).

Table 7.10: Losses comparisson in the urban MV grid scenario.

	Curtailment	**Storage**
Curtailed energy	6879 MWh	-
Line and transformer losses	2695 MWh	3333 MWh
Storage losses	-	1102 MWh
Total energy losses	9574 MWh	4435 MWh

Chapter 8

Automatic conventional grid upgrade

Within this master's thesis, two different ways are considered to solve grid problems, such as overvoltages, undervoltages or components overloads. On the one hand, there is the conventional grid extension, i.e. when it is expected that a line is not strong enough to avoid, for instance, large voltage drops, these lines are upgraded. On the other hand, several active distribution network strategies such as tap changing transformers or battery installations can be used to reduce these problems of the current network without changing grid components.

8.1 Automatic planning algorithm

To address the first part, an algorithm for an automatic conventional grid upgrade has been developed in MATLAB. There is available bibliography on the topic [13]. The procedure for this algorithm starts as follows. A simulation is carried out in DPG.sim while at the same time the results and the power flows are stored and can be retrieved from MATLAB. The maximum bus voltages and component loadings will be saved in MATLAB so the variables are first initialised. Then, every time a larger overvoltage/overloading than the last saved is retrieved, the power flows and component states at that time step of the simulation are stored (and therefore the previous ones overwritten). At the end of the simulation, the results of the worst-case time step will be available.

There are three non-desirable results to be checked: overvoltages, line overloading and transformer overloading. The lines and transformer loadings will be checked in first place as they will have to change in any case and this change will lead to a change the power flows and therefore the voltages will have to be recalculated.

The saved power flow data is used to evaluate the suitability of the new grid components (retrieved from the providers' lists). These are tested before the actual change: no grid component will be changed if it does not solve the overvoltage or overloading. The criteria used by the algorithm in order to select an appropriate line from the provider's list is:

- The line electrical resistance cannot be larger than the current one.
- Maximum line capacity must at least withstand the currently occurring maximum line current.

The criteria for the transformers is to fulfill the voltage ratings at both sides and that their maximum permissible power cannot be smaller than the current loading. As transformers will usually be changed due to overloadings, these criteria do not include an impedance check.

The next step will be to check whether still more components have to be upgraded due to overvoltages or undervoltages. To address this problem, the algorithm will look for the line with greater voltage drop, but only for the ones located between the bus with the biggest overvoltage and the network feeder. This is implemented with a recursive search tree algorithm. In order to change as few lines as possible, this line will be substituted with either a line with less resistance that solves the voltage problem (if found), or the largest line (in terms of cross-section). The procedure to select the appropriate new component is performed as follows:

1. The current component is searched in the providers' files. In case it is found, and as the components are sorted by size, the next line or transformer in the file that fulfills the criteria described before will be selected. If the selected component does not solve the problem to be avoided, then the next line in the list will be selected (lines are ordered by size)
2. Otherwise (current component not found), the algorithm will list one appropriate component (if found) of each provider file, plot worst-case voltages and loadings, and let the user choose the one he finds more convenient.

A summary of the functionality of the code is described in Fig. 8.1. The two sub-processes in charge of changing problematic components are also detailed in Fig. 8.2 and 8.3.

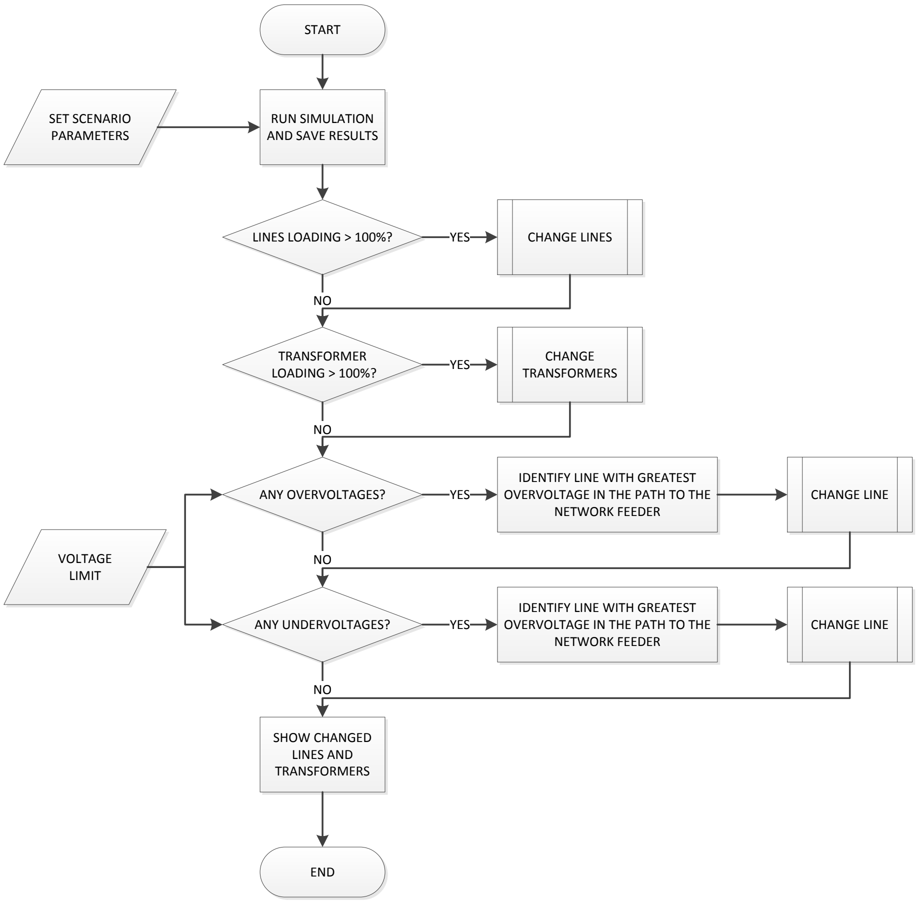

Figure 8.1: Main steps of the automatic grid upgrade code.

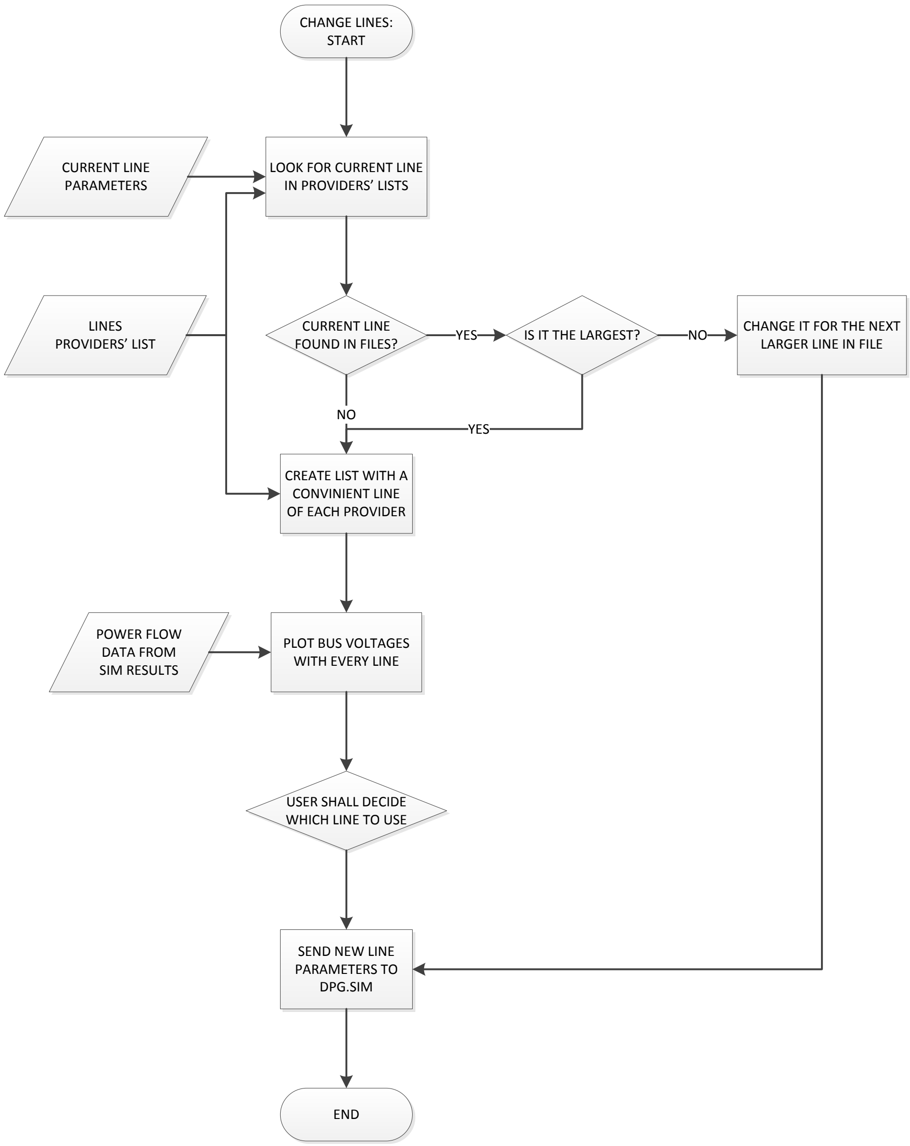

Figure 8.2: Steps to change a specific lines.

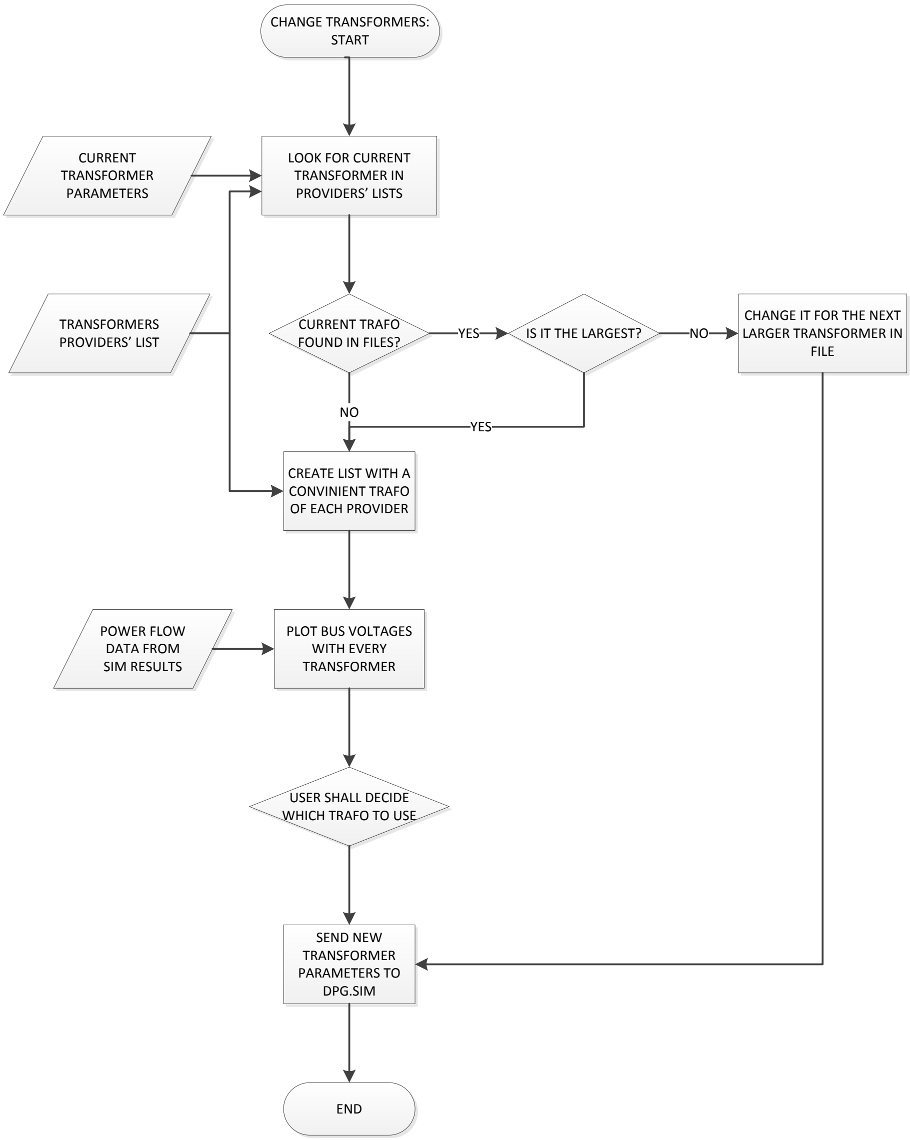

Figure 8.3: Steps to change a specific transformer.

Table 8.1: Line parameters of the upgraded line.

	Resistance (Ω/km)	**Reactance (Ω/km)**	**Capacitance (μF/km)**	$\mathbf{I}_{max}$ **(A)**
Old line	0.579	0.367	0.159	310
New line	0.146	0.107	0.303	347.6

8.2 Simulation example

The algorithm for a conventional grid reinforcement is used within this chapter to see the resulting grid of the MV rural benchmark grid used in the previous chapters with a conventional grid upgrade.

The voltage limit is set to 10% and two files with aluminum and copper MV line parameters of different cross sections are provided to the algorithm when this data is needed. The resulting grid has an upgraded line between bus 416001 and bus 416005 (the location of the buses can be seen in Fig. 4.2). The previous and new parameters of this line are given in Table 8.1 and the new worst-case voltages for each grid bus can be found in Fig. 8.4. These plots are shown in MATLAB for the user to decide which line to use but in this case both lines (Al and Cu) yield similar voltage results, so both options are possible. The aluminum line is chosen because it has higher current rating and the new voltage time-series is shown in Fig. 8.5.

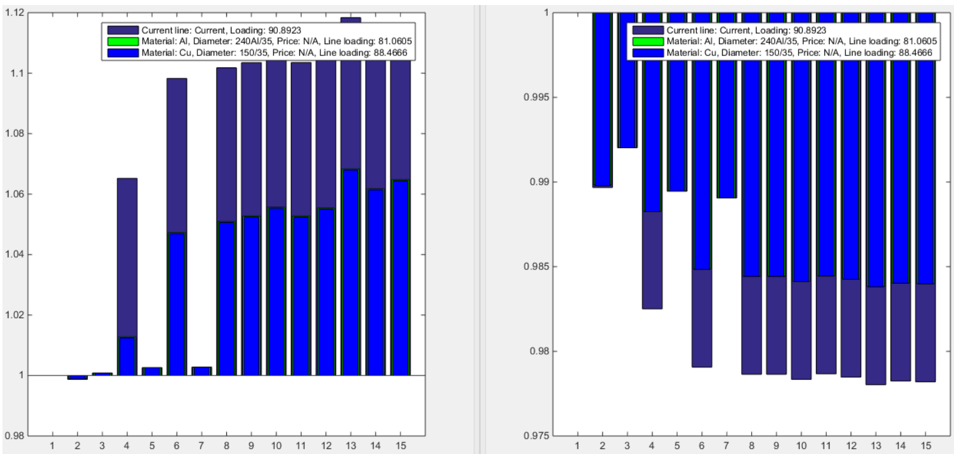

Figure 8.4: MATLAB plots with worst-case voltages of Al and Cu lines.

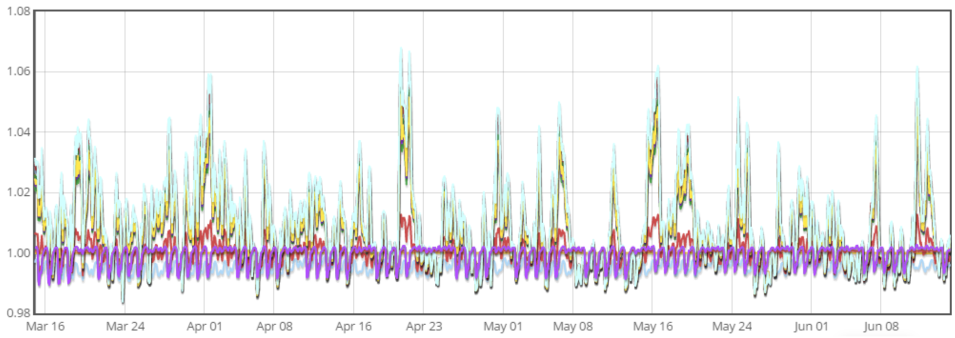

Figure 8.5: Voltage time-series of MV rural grid with conventional grid extension.

Chapter 9

Conclusions and outlook

As previously introduced and shown within the thesis, electrical utilities and DSOs are facing technical challenges such as overvoltage, overloadings or unwanted backflows into the network feeders due to the increased share of generated energy from renewable sources. Distribution networks were not designed to host generation and the DSOs cannot freely decide on the connection time of distributed generation, increasing uncertainties for the DSO's network planning and the need for energy balancing to ensure power quality. Traditionally, grid infrastructure would need to be reinforced to increase the RES hosting capacity although the use of innovative smart grid approaches allow to reduce or even avoid the associated cost of grid reinforcement.

9.1 Summary of the thesis

This thesis contributes in the two mentioned directions to increase RES hosting capacity with the use of DPG.sim, time-simulations software for network planning developed by Adaptricity.

As for the traditional network planning, an automatic grid reinforcement algorithm is designed to be used with DPG.sim. The algorithm will automatically decide, with help of the simulation results and a list of the suppliers' components, which of the current grid elements need to be upgraded to ensure power quality. For instance, given the bus with the biggest overvoltage, the algorithm will look for the line with the greatest voltage drop between the bus and the network feeder, and select the appropriate line from a supplier list with which to replace the current line. The simulation example for a MV grid is also included.

As for the smart grid approaches, a study of three benchmark grids has been carried out to test the performance of SmartGrid strategies on three different grid topologies. This implied in the first place the parametrization of the benchmark grids, trying to use realistic setups and testing how different locations and sizes can change the results of similar parameterizations. Once the benchmark grids are parametrized so that they cannot host the dispersed generation, the different smart-grid strategies are designed: sizing and location of batteries, curtailment of surplus power, OLTC transformers and reactive power control.

The study shows not only how much energy needs to be curtailed for the grid to be under normal conditions but also how the grid hosting capacity can be enlarged with SmartGrid approaches, including the parametrization and sizing of these. Some interesting insights of the controllers operation, interaction and sizing come out of the study: batteries will need much more storage capacity if they need to store wind energy and if they are behind a weak line, as they may not be able to fully discharge overnight. Again, communication between batteries and RES sources would be desirable: it would allow to only charge excess energy from the source instead of using a fixed battery charging power.

9.2 Future work

In the first place, data sampling could be applied for the load and generation profiles: the study was implemented with the aggregated values of load and generation in all the prosumers, whereas in reality each prosumer has a different load/generation profile and the sum of all profiles should match the aggregated values. The study could be carried out under these conditions, but further sampling and randomisation would be interesting. As for randomisation, DPG.sim allows for stochastic datasets that can vary from one simulation to another. This was kept for further work and a seed was used for obtaining fixed numerical values in order to make the simulations reproducible.

A sensitivity analysis of the grid to see how much dispersed generation the grids can host and develop system sizing rules would also be of interest. Moreover, an economical analysis to decide which approach is best for each grid would be even more complete than only a technical analysis.

Finally, the differences between radial grids and grids with rings was not part of this study but could also be of interest.

Appendix A

Time-series profiles

The load and generation profiles used within the study are included below. Fig. A.1 shows the load profiles from KommEnergie GmbH used for households (top), industrial (middle) and commercial (bottom) loads and Fig. A.2 shows the wind and PV time-series profiles from Tennet control area in 2010.

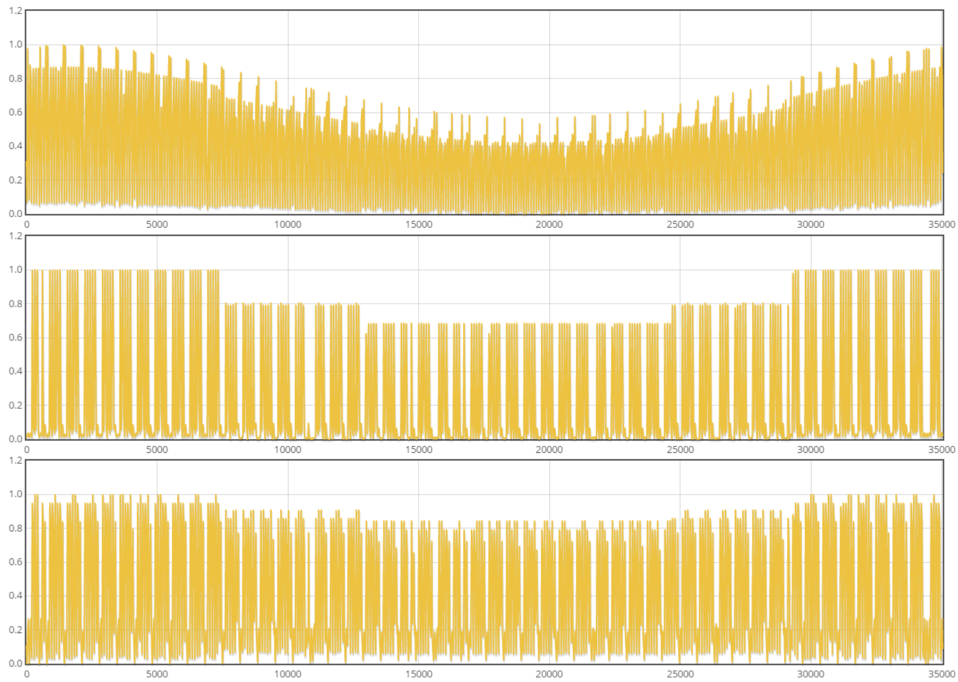

Figure A.1: Standard load profile H0 (top), G1 (middle), G2 (bottom) from KommEnergie GmbH data.

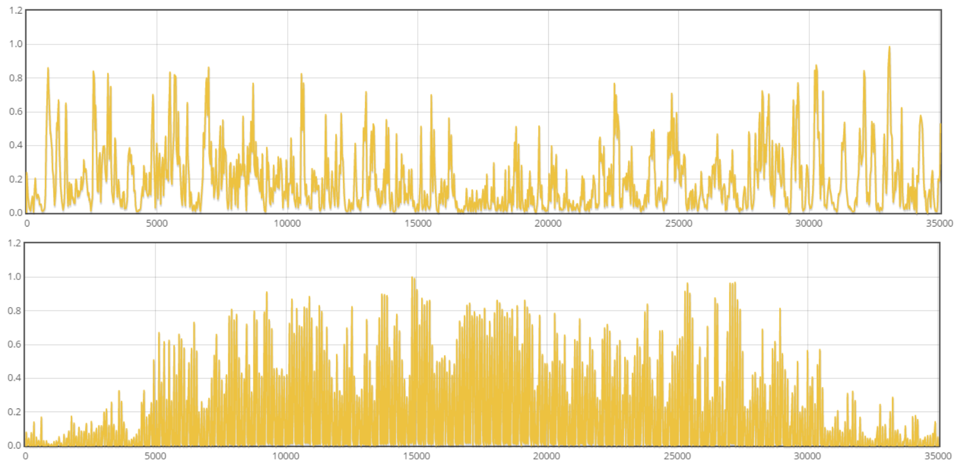

Figure A.2: Aggregated wind (top) and PV (bottom) generation from TenneT control area over 1 year.

Bibliography

[1] EUROSTAT. Energy from renewable sources. Available from: http://ec.europa.eu/eurostat/statistics-explained/index.php/Energy_from_renewable_sources, March 2015. [Online; accessed 23th June 2015].

[2] REN21 SECRETARIAT. Renewables 2015 global status report. Technical report, Renewable Energy Policy Network for the 21st Century, Paris, 2015. Available from: http://www.ren21.net/wp-content/uploads/2015/06/REN12-GSR2015_Onlinebook_low1.pdf.

[3] B. ERNST and B. ENGEL. Grid integration of distributed PV generation. In *Power and Energy Society General Meeting, 2012 IEEE*, pages 1–7, July 2012.

[4] T. BEACH, A. KOZINDA, and V. RAO. Advanced inverters for distributed PV: Latent opportunities for localized reactive power compensation. *Cal x Clean Coalition Energy C226*, October 2013. Available from: http://www.clean-coalition.org/site/wp-content/uploads/2013/10/CC_PV_AI_Paper_Final_Draft_v2.5_05_13_2013_AK.pdf.

[5] K. DALLMER-ZERBE and B. WILLE-HAUSSMANN. Distribution grid planning with decentralized reactive power control and OLTC. In *Zukünftige Stromnetze für Erneuerbare Energien*, Berlin, January 2014. Ostbayerische Technologie-Transfer-Institut (OTTI).

[6] M. KOLLER, T. BORSCHE, A. ULBIG, and G. ANDERSSON. Review of grid applications with the Zurich 1 MW battery energy storage system. *Electric Power Systems Research*, 120:128–135, 2015.

[7] X. LI, T. BORSCHE, and G. ANDERSSON. PV integration in low-voltage feeders with demand response. In *Towards Future Power Systems and Emerging Technologies*, Eindhoven, June 2015. PowerTech, IEEE Power & Energy Society. Available from: http://arxiv.org/pdf/1408.1602v1.pdf.

[8] S. KOCH, A. ULBIG, and F. FERRUCI. An innovative software platform for simulation and optimization of active distribution grids for DSOs and SmartGrid researchers. In *Challenges of implementing Active Distribution System Management*, number 0330, Rome, June 2014. CIRED Workshop 2014. Available from: `http://adaptricity.com/files/publications/adaptricity_cired_2014.pdf`.

[9] S. PAPATHANASSIOU, N. HATZIARGYRIOU, and K. STRUNZ. A benchmark low voltage microgrid network. *Proceedings of the CIGRE symposium: power systems with dispersed generation, Athens, 13-16 April 2005*, pages 1–8, 2005.

[10] K. RUDION, A. ORTHS, Z.A. STYCZYNSKI, and K. STRUNZ. Design of benchmark of medium voltage distribution network for investigation of DG integration. In *Power Engineering Society General Meeting, 2006. IEEE*, pages 6 pp.–, 2006.

[11] Q. GEMINE, D. ERNST, and B. CORNÉLUSSE. Active network management for electrical distribution systems: problem formulation and benchmark. *Proceedings of the 9th French Meeting on Planning, Decision Making and Learning, LiÃ¨ge, Belgium, May 12-13, 2014*, 2014.

[12] H MARKIEWICZ and KLAJN A. Standard EN 50160-voltage characteristics in public distribution systems. *Report: Leonardo Power Quality Initiative (LPQI), The European Commission, Wroclaw University of Technology*, July 2004.

[13] K. DALLMER-ZERBE. Automatisierte verteilnetzplanung unter berücksichtigung von Smart Grid lösungen. In *Zukünftige Stromnetze für Erneuerbare Energien*, Berlin, January 2015. Ostbayerische Technologie-Transfer-Institut (OTTI).